5 Solar Thermal Power Plants

The term "solar thermal power plant" comprises power plants which first convert solar radiation into heat. The resulting thermal energy is subsequently transformed into mechanical energy by a thermal engine, and then converted into electricity. For thermodynamic reasons high temperatures are required to achieve the utmost efficiency. Such high temperatures are reached by increasing the energy flux density of the solar radiation incident on a collector. In this respect, we refer to concentrated radiation or concentrating collectors. As an alternative, with regard to technical/economic optimisation of the overall system, also lower temperatures, resulting in considerably reduced costs may be desired in some cases. However, such concepts imply the use of large-surface cost-efficient collectors. The above mentioned framework conditions give rise to a whole series of different solar thermal power plant concepts.

According to the type of solar radiation concentration, solar thermal power plants are subdivided into concentrating and non-concentrating systems. The former are further subdivided into point and line focussing systems. In addition, further differentiations can be made, e.g. according to the type of receiver of the solar radiation, the heat transfer media and the heat storage system (if applicable) or the additional firing based on fossil fuel energy; however, to structure this chapter as clear as possible, these differentiations have not been considered here.

The term "concentrating systems" covers primarily the following power plant concepts:

- solar tower power plants (i.e. central receiver systems) as point focussing power plants,
- dish/Stirling systems as point focussing power plants and
- parabolic trough and Fresnel trough power plants as line focussing power plants.

Non-concentrating systems include the concepts of solar updraft tower power plants and solar pond power plants.

The different options are explained and discussed in the following sections. However, emphasis has been laid on those technologies and processes which seem most promising to contribute substantially to cover the given electricity demand on a global scale.

Concentrating collectors can reach temperature levels similar to that of existing fossil-fuel fired thermal power stations (e.g. power plants fired with coal or natural gas). Consequently, the various components required for the actual thermal energy conversion process (including, for instance, turbine and generator) are

already state-of-the-art technology. Due to this, within the following sections, only the solar-specific part of such power plants is discussed in detail.

5.1 Principles

Basically, the process of solar thermal power generation is realised within the following steps:

- concentrating solar radiation by means of a collector system;
- increasing radiation flux density (i.e. concentrating of the solar radiation onto a receiver), if applicable;
- absorption of the solar radiation (i.e. conversion of the radiation energy into thermal energy (i.e. heat) inside the receiver);
- transfer of thermal energy to an energy conversion unit;
- conversion of thermal energy into mechanical energy using a thermal engine (e.g. steam turbine);
- conversion of mechanical energy into electrical energy using a generator.

Fig. 5.1 illustrates the general energy conversion chain of such a solar thermal power generation plant. Selected aspects of this kind of solar energy conversion are discussed below.

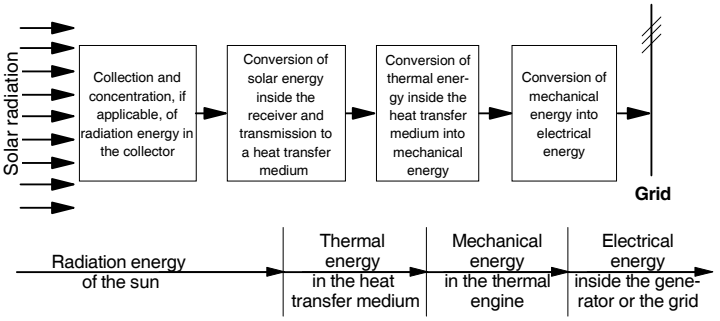

Fig. 5.1 Energy conversion chain of solar thermal power generation

5.1.1 Radiation concentration

Radiation concentration is necessary if higher temperatures than those generated by flat-plate collectors are required. The concentration of solar radiation is described by the concentration ratio. It is defined according to two different methods:

- On the one hand, concentration ratio C can be determined solely geometrically (C_{geom}), describing the ratio of the solar aperture surface A_{ap} to the absorber surface A_{abs} (Equation (5.1)); also, the explanations within this chapter are based

on this definition. Thus, the concentration ratio of a typical parabolic through collector of an aperture width of 5.8 m and an absorber tube diameter of 70 mm amounts to approximately 26. With regard to parabolic through collectors, sometimes the ratio of aperture width to absorber tube diameter is referred to as concentration ratio; this quantity differs from the concentration ratio defined by Equation (5.1) by factor π.

$$C = C_{geom} = \frac{A_{ap}}{A_{abs}} \tag{5.1}$$

- On the other hand, the concentration ratio C can be defined as the ratio of the radiation flux density G_{ap} at the aperture level and the corresponding value G_{abs} of the absorber (C_{flux}, Equation (5.2)). However, this definition is only mentioned here to complete the picture.

$$C = C_{flux} = \frac{G_{ap}}{G_{abs}} \tag{5.2}$$

On the basis of the second fundamental theorem of thermodynamics the maximum possible concentration ratios for two-dimensional (parabolic trough-type) and three-dimensional (e.g. paraboloids of revolution) concentrators can be deduced /5-1/. For this purpose the "acceptance angle" $2\theta_a$ is required. This angle covers the entire angular field of solar beams to be focussed by the collector, without having to move the collector or part of it.

For single-axis concentrators (e.g. parabolic trough), for instance, the maximum concentration ratio $C_{ideal,2D}$ for a given acceptance semi-angle θ_a is calculated according to Equation (5.3).

$$C_{ideal,2D} = \frac{1}{\sin\theta_a} \tag{5.3}$$

For two-axis concentrators (e.g. paraboloids of revolution) the maximum concentration ratio $C_{ideal,3D}$ is calculated according to Equation (5.4).

$$C_{ideal,3D} = \frac{1}{(\sin\theta_a)^2} \tag{5.4}$$

Since on the earth's surface the acceptance angle $2\theta_a$ for the sun amounts to 0.53° or 9.3 mrad, maximum ideal concentration factors of 213 are determined for two-dimensional geometries (line focussing parabolic through) and of 45,300 for three-dimensional (point focussing) geometries.

However, in practice the acceptance angle of the concentrator must be increased so that the actual achievable concentration ratio is necessarily considerably reduced. This is due to the following aspects:

- Tracking errors, geometric reflections as well as imperfect orientation of the receiver lead to acceptance angles which are considerably bigger than the aperture angle of the sun.
- The applied mirrors are imperfect and expand the reflected beam.
- Atmospheric scattering expands the efficient aperture angle of the sun far beyond the ideal geometric value of the acceptance semi-angle of approximately 4.7 mrad.

Radiation concentration is aimed at increasing the possible absorber temperature and consequently the exergy of the concentrated heat. In addition, absorber surfaces may be of smaller design due to the concentrated solar radiation. It is thus easier to reduce the inevitable thermal losses due to radiation, convection and heat conduction. In case of absorbers of parabolic through collectors, this is achieved by evacuated cladding tubes and by an absorber coating with a low emission coefficient within the relevant wavelength range. Fig. 5.2 shows the impact of the concentration ratio on the collector efficiency η_{Coll} over the absorber temperature θ_{abs} for two different emission coefficients ε of the absorber (left ε_{abs} = 1, right ε_{abs} = 0.08).

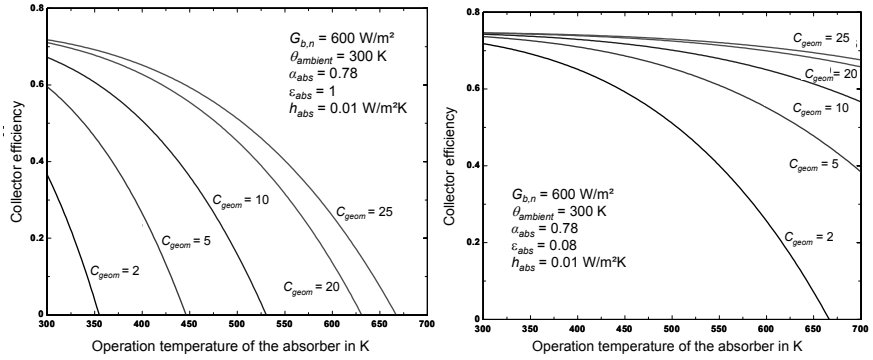

Fig. 5.2 Correlation between collector efficiency η_{Coll} and operation temperature of the absorber θ_{abs} as well as geometric concentration factor C_{geom} (left for an absorber of an emission coefficient ε_{abs} = 1 ("black body radiator"), right for ε_{abs} = 0.08, a practically achievable value; for the sake of simplicity a constant intercept factor (i.e. ratio of incident to reflected radiation) of 0.96 has been assumed; $G_{b,n}$ describes the direct normal radiation; α_{abs} is the absorption coefficient of the absorber; h_{abs} is the thermal loss coefficient of the absorber)

Since direct concentration by diffraction or refraction can only be performed by rigid, transparent materials (e.g. glass lenses), characterised by high costs, this option has not been applied on a large scale for economic reasons. Reflecting surfaces have proven most cost-efficient since they reflect the almost parallel

incident radiation onto a certain point or line. Parabola profiles show these properties (Fig. 5.3 a)). To achieve the highest possible concentration ratio – i.e. the ratio of reflector surface to absorber surface should be very high for economic reasons – the profiles are designed as rotational solids (Fig. 5.3 e)). As an alternative, the reflecting profile can also be extruded, so that the focus is not of point but of line-shape. These possibilities are outlined in Fig. 5.3 c).

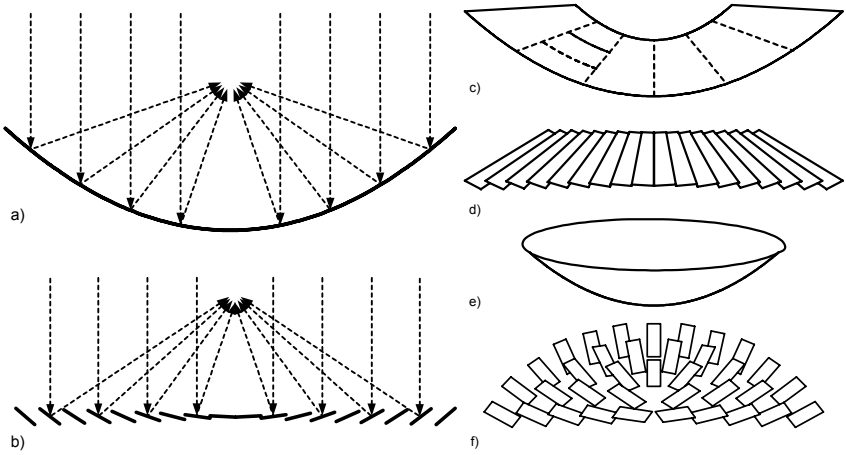

Fig. 5.3 Parabola profiles for radiation concentration (a) parabola profile with ray path, b) segmented parabola profile (Fresnel) with ray path, c) and d) profiles extruded from profiles a) and b), e) and f) rotational solids of profiles a) and b))

The more flat the parabola, the more distant is the focal point (or the focal plane of the image of the sun) from the apex of the parabola. When compared to steeper parabola profiles, flat profiles are characterised by a lower ratio of reflector surface to aperture surface (i.e. effective collector surface). Specific material consumption is thus reduced. Nevertheless, a certain depth of the profile and considerable technical effort are inevitable. As an alternative, segmented parabola profiles – also referred to as Fresnel profiles – are applied. The parabola profile is subdivided into smaller segments of the same slope at the same point as the profile, but located on the same level. Due to blocking of incident and reflected radiation, reflection efficiencies (i.e. ratio of radiation on aperture surface and concentrated radiation) are generally lower than for realised parabola profiles. Fig. 5.3 d) shows schematic representations of such segmented profiles for extruded profiles and Fig. 5.3 f) contains a schematic representation of rotational solids.

Rotation profiles present the advantage of generally higher concentration factors and thus higher process temperatures. However, these concentrators need two-axis sun-tracking requiring greater technical efforts. Line-focussing systems only require single-axis tracking and result in lower process temperatures and efficiencies.

In the following, plants equipped with rotation parabola profiles are referred to as dish/Stirling systems or parabola power plants, and large-scale plants with segmented rotation profiles as solar tower power plants (due to the focal plane being located on a tower). In case of line-focussing plants equipped with extruded parabola profiles the common technical terms are parabolic trough power plants or linear Fresnel collector power plants.

Besides the optical properties of the material applied for the reflector, achievable efficiencies are largely influenced by the geometry of the reflectors and the precision of the sun-tracking system. In practice, mainly optical measuring methods are used to assess the concentrator quality and the performance.

Typical concentration factors and parameters of different solar power generation technologies applying concentrating collectors are summarised in Table 5.1. To allow for a comparison, technical data of non-concentrating solar-thermal power plants have also been added.

Table 5.1 Concentration factors and technical parameters of selected solar thermal power generation technologies

	Solar tower	Dish/Stirling	Parabolic trough	Fresnel reflector	Solar pond	Solar updraft tower
Typical capacity in MW	30 – 200	0.01 – 1[a]	10 – 200[c]	10 – 200[c]	0.2 – 5	30 – 200[c]
Real capacity in MW	10	0.025	80	0.3[d]	5	0.05
Concentration factor	600 – 1,000	up to 3,000	50 – 90	25 – 50	1	1
Efficiency[b] in %	10 – 28	15 – 25	10 – 23	9 – 17[d]	1	0.7 – 1.2
Operation mode	grid	grid/island	grid	grid	grid	grid
Development status[e]	+	+	++	0	+	+

[a] by interconnection of many individual plants within a farm; [b] conversion of radiation energy into electrical energy, annual average is site-specific; [c] assuming a solar multiple of 1.0; [d] incorporated into a conventional power station; [e] 0 successful operation of demonstration plants, + successful continuous operation of demonstration plants, ++ commercial plants in operation.

5.1.2 Radiation absorption

All materials absorb part of the incident solar radiation. The absorbed incident radiation causes atoms of the material to vibrate, whereby heat is generated. This heat is either transferred within the absorbing material by heat conduction and/or released by heat radiation or convection back to the atmosphere.

The major portion of solar radiation consists of visible light (Fig. 2.8); i.e. the short-wave portion of radiation is predominant (Chapter 2.2). The distribution of luminosity of the different wavelengths corresponds approximately to that of a black body radiator of a temperature of approximately 5,700 K. In contrast, with regard to the temperatures relevant to solar thermal plants (approx. 100 to 1,000 °C) bodies radiate mainly medium and short-wave radiation (Wien's Law). When observing only a small spectral range, the absorption coefficient and emission coefficient are identical (Kirchhoff's Law). However, suitable "selective" coatings ensure that short-wave sunlight is well absorbed while (long-wave) heat

radiation is inhibited. Such absorber materials are thus characterised by high absorption coefficients α_{abs} with regard to solar radiation and low emission coefficients ε_{abs} in terms of long-wave heat radiation: they are sometimes also referred to as α/ε coatings (see Fig. 5.2).

5.1.3 High-temperature heat storage

Solar radiation is an energy source whose intensity varies deterministically due to the rotation of the earth (day/night) and stochastically as a result of actual meteorological influences (clouds, aerosols, etc.). To compensate for such fluctuations thermal storages can be applied.

In this respect, heat transfer medium storage, mass storage and storage of phase-change material are distinguished.

- In case of storage of the heat transfer medium, it is intermediately stored in thermally insulated containers. However, this implies that the heat transfer medium is inexpensively available and has a high volume-specific heat capacity to minimise container costs. To date, thermal oil and molten salt containers have been applied; however, also water/steam accumulators have been planned. The advantage of this storage mode is the constant temperature of the hot heat transfer medium, which is only reduced by heat losses of the storage tank (and thus is a function of the storage period, the container surface and the insulation).
- In case of mass storage, the heat transfer medium thermally charges a second material of a high heat capacity. For this purpose a good heat transfer (i.e. large surfaces and high heat transmission coefficients) must be provided between the heat transfer medium and the storage material, to ensure the required driving temperature difference and to reduce the ensuing exergy loss of heat transmission. Mass storages are applied if the heat transfer medium itself is too expensive (e.g. synthetic heat transfer oil) or difficult to store (e.g. depressurised air). For mass storages the following combinations are applied: thermal oil/concrete, thermal oil/molten salt, steam/oil-sand and air/ceramics bricks. Mass storage offers the advantage of very inexpensive storage material. However, it also presents the disadvantage that in addition to the common heat loss of the storage tank also an exergy loss occurs during double heat transmission when charging and discharging the storage material.
- Within storage tanks with phase-change material steam is condensed isothermally, so that a storage material (e.g. salts such as NaCl, $NaNO_3$, KOH) is solidified/melted isothermally. Also in this case, an exergy loss occurs due to double heat transmission. Moreover, such phase-change materials are still very expensive.

Table 5.2 shows the thermodynamic data of selected storage media. One characteristic parameter is the thermal penetration coefficient a_{th}. According to Equation

(5.5) a_{th} it is defined as the root of the product of thermal conductivity λ, density of the storage medium ρ_{SM} and specific heat capacity c_p.

$$a_{th} = \sqrt{\lambda \cdot \rho_{SM} \cdot c_p} \tag{5.5}$$

Table 5.2 Parameters of different storage materials (standard values)

	Maximum temperature	Thermal conductivity	Density	Specific heat capacity	Thermal penetration coefficient
	in °C	in W/(m K)	in kg/m^3	in J/(kg K)	in Ws$^{1/2}$/Km²
Silicone oil	400	0.1	970[a]	2,100	450
Mineral oil	300	0.12	900[a]	2,600	530
Molten sodium chloride	450	0.57	927[b]	1,500	890
Insulating bricks	700	0.9[c]	Approx. 1,000[d]	950	925
Reinf. concrete	400	1.5	2,500	850	1785
Construction steel	700	40	7,900	430	11,700

Spec. Specific; Reinf. Reinforced; Approx. approximately; [a] at 20 °C; [b] at melting point; [c] 0.18 to 1.6 W/(mK); [d] between approximately 800 to 1,200 kg/m³.

5.1.4 Thermodynamic cycles

The exergy of heat can be utilised by closed or open cycles. In these processes a working medium undergoes a series of state changes which are either caused by heat exchange or performance of work.

- If the initial state is identical to the final state, so that the working medium could undergo the same process again, the process is referred to as a "closed cycle" (Fig. 5.4).

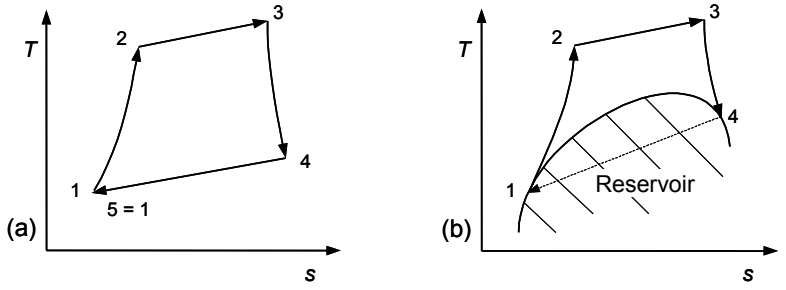

Fig. 5.4 Temperature/entropy-diagram (*T,s*-diagram) of a closed (left, (a)) and an open cycle (right, (b)) (the arrows refer to the direction the cycles performed)

- If the working medium is part of an "inexhaustible" reservoir (e.g. ambient air) and its final state is different from the initial state, the process is referred to as an "open cycle" (Fig. 5.4); yet, strictly speaking, such a process is also closed since the last state change takes place outside of the actual process, namely within the "inexhaustible" reservoir.

In the following such cycles are illustrated by means of temperature/entropy-diagrams. These representations offer the advantage, that both isothermal (i.e. constant temperatures) as well as isentropic (i.e. constant entropy) state changes can be represented as straight lines (Fig. 5.4 (a)) /5-2/.

- Within the Carnot cycle the entire exergy is extracted from the supplied heat so that its full working capacity becomes useful. This cycle consists of isentropic compression/decompression (i.e. performance of pressure change work) and isothermal heat supply and dissipation. The Carnot cycle is an ideal comparative process; however, mainly the isentropic compression/expansion cannot be put into practice (Fig. 5.5 (a)).
- The Ericson cycle represents the first technical approach to an ideal Carnot cycle; isobaric compression and expansion substitute isentropic compression/decompression. Within this cycle addition and evacuation of heat is supported by internal heat transmission (Fig. 5.5 (b)).
- The Stirling cycle is similar to the Ericson cycle. However, compression/decompression is isochore (i.e. density remains constant) (Fig. 5.5 (c)).

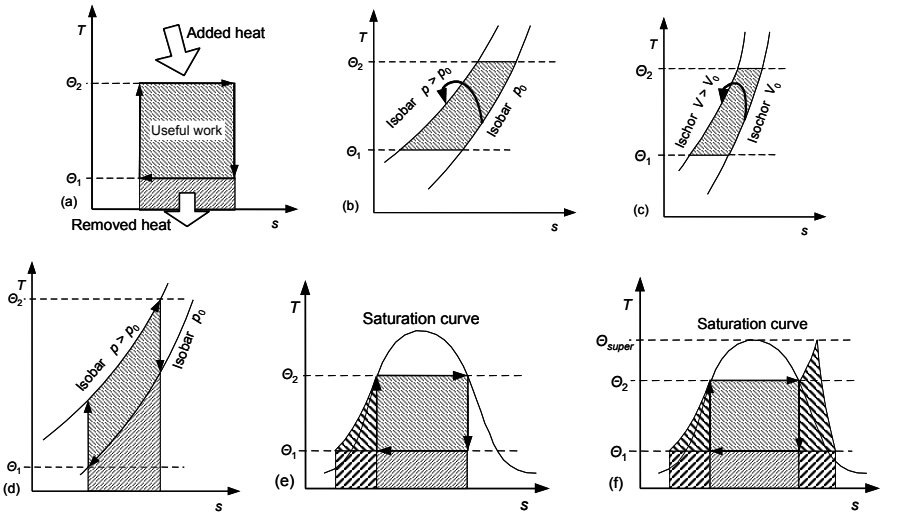

Fig. 5.5 Temperature/entropy diagram (*T,s*-diagram) of various cycles ((a) Carnot cycle, (b) Ericson cycle, (c) Stirling cycle, (d) Joule cycle, (e) Clausius-Rankine cycle, (f) Clausius-Rankine cycle with superheating) (*p* pressure, *V* volume, *T,θ* Temperature, *s* entropy)

- The Joule cycle is composed of isentropic compression, isobaric heat addition (combustion), isentropic expansion and isobaric heat dissipation (Fig. 5.5 (d)).

- The Clausius-Rankine cycle (steam power cycle/two phase cycle) makes use of the phase transformation of matters. Such phase transformations correspond to isothermal heat addition and large additions of specific volume. Their technical application is easy (isotropic compression/decompression, isothermal heat addition and dissipation). This is why such processes were first technically applied (Fig. 5.5 (e), (f)).

For current industrial applications Joule and Rankine cycles are most commonly applied.

- For the Joule cycle the working medium "ambient air" is aspirated and compressed prior to adding heat. Heat can either be added by caloric devices or internal combustion (e.g. by combustion of natural gas). For solar applications heat is transferred directly from the absorber to the working medium of the energy conversion process. The volumetric absorber itself has a very large surface to benefit both heat transfer and radiation absorption. Since pressurised air is used as working medium such an absorber must be of closed design. Indirect heat addition, for instance by means of a heat transfer medium, is disadvantageous since the working medium air only has a poor thermal conductivity and thus requires large surfaces for heat transmission.
- The Clausius-Rankine cycle, by contrast, requires a phase change medium to allow for isothermal heat addition. In most cases water is applied, but there are also processes using organic working media for low-temperature applications (so-called Organic Rankine Cycles (ORC)). At the beginning, the liquid working medium is highly pressurised and undergoes a phase change while heat is added. The now gaseous material is subsequently expanded, possibly after further heat has been added. Afterwards condensation is performed under low pressure while heat is dissipated.

All above-mentioned cycles have in common that heat is first applied to increase the volume flow of a gaseous working medium. Subsequently, during its expansion, this volume flow performs mechanical work in pressure engines, which can either be designed as oscillating machines of varying working volume (i.e. reciprocating engines) or as machines with stationary flow (i.e. turbo-machines or turbines). For large-scale power plants dealing with large volume flows almost exclusively turbo-engines are applied.

Turbines are referred to as turbo-engines which first transform the potential energy of a flowing working medium into kinetic energy and afterwards into mechanical energy of the rotating turbine shaft. The medium flows through the turbine either axially or radially, causing it to rotate. A stator whose blades form nozzles causes the working medium to first expand and at the same time accelerates the rotor. Inside the rotor coupled to the turbine shaft the kinetic energy of the working medium is subsequently converted into shaft torque. The combination of rotor and stator is referred to as turbine stage; for instance, in large turbines up to sixty subsequent stages are implemented. Inevitable friction, inconvertible kinetic energy at the turbine exit and so-called gap leakages are considered to measure

the efficiency of a turbine; current steam turbines reach efficiencies above 40 %, while those of gas turbines even exceed 55 %.

5.2 Solar tower power stations

Within solar tower power plants (also called "central receiver systems") mirrors tracking the course of the sun in two axes, so-called heliostats (Greek term for "immobile sun"), reflect the direct solar radiation onto a receiver, centrally positioned on a tower. There, radiation energy is converted into heat and transferred to a heat transfer medium (e.g. air, liquid salt, water/steam). This heat drives a conventional thermal engine. To ensure constant parameters and a constant flow of the working medium also at times of varying solar radiation, either a heat storage can be incorporated into the system or additional firing using e.g. fossil fuels (like natural gas) or renewable energy (like biofuels) can be used. Such systems are described in detail below.

5.2.1 Technical description

In the following the technology of solar tower power plants including all related components are described.

5.2.1.1 System components

Heliostats. Heliostats are reflecting surfaces provided with a two-axis tracking system which ensures that the incident sunlight is reflected towards a certain target point throughout the day. In addition, heliostats commonly concentrate sunlight by means of a curved surface or an appropriate orientation of partial areas, so that radiation flux density is increased.

Heliostats consist of the reflector surface (e.g. mirrors, mirror facets, other sunlight-reflecting surfaces), a sun-tracking system provided with drive motors, foundations and control electronics. The individual heliostat's orientation is commonly calculated on the basis of the current position of the sun, the spatial position of the heliostats and the target point. The target value is communicated electronically to the respective drive motors via a communication line. This information is updated every few seconds. The concentrator surface size of currently available heliostats varies between 20 and 150 m^2; to date, the largest heliostat surface amounts to 200 m².

The heliostat field accounts for about half the cost of the solar components of such a power plant. This is why tremendous efforts have been made to develop heliostats of good optical quality, high reliability, long technical life and low specific costs. Due to economic considerations there is a tendency to manufacture

heliostats with surfaces ranging between 100 and 200 m^2 and possibly beyond. However, there are also approaches to manufacture smaller heliostats to reduce costs by efficient mass-production.

Heliostats are usually centrally controlled and centrally supplied with electrical energy. As an alternative, autonomous heliostats have been developed which are controlled locally. There, the energy required for the control processor and the drives is provided by photovoltaic cells mounted parallel to the reflector surface.

The heliostats are individually controlled in order to control the radiation flux density on the receiver. For this reason not all of the heliostats are focussed on the same point of the receiver; their control rather ensures a smooth flux distribution over the entire receiver surface.

Based on the developments of the last few years, faceted glass/metal heliostats and membrane heliostats are distinguished (Fig. 5.6). These types are described below.

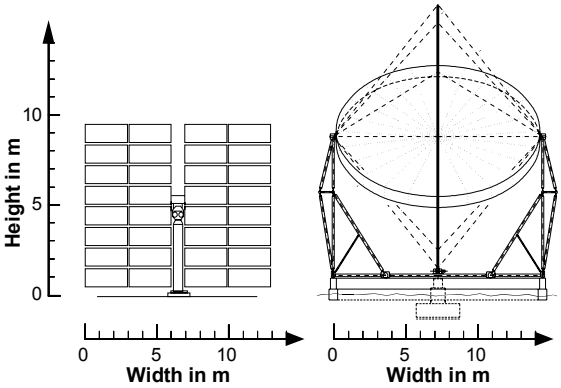

Fig. 5.6 Faceted glass/metal heliostat (left) and metal membrane heliostat (right) /5-3/

Faceted heliostats. Usually, faceted heliostats consist of a certain number of reflecting facets mounted on lattice work which in turn is positioned on a mounting tube. The facets are commonly designed as individual mirrors of sizes between 2 and 4 m^2. The orientation of the individual mirrors on top of the mounting structure (referred to as "canting") is different for every heliostat within the heliostat field, and thus results very expensive. The heliostats are usually tracking in two axes positioned vertically to each other (commonly mounting tube and vertical main axis), according to the desired azimuth and elevation angle. Mostly to reduce canting efforts and the number of individual drives, currently wide facetted heliostats are proposed. The glass/metal heliostat illustrated in Fig. 5.6 (left) as an example has a concentrator width of 12.8 m and a height of 8.94 m. The size of the individual facets is 3 by 1.1 m each. The total weight without foundation amounts to scarcely 5.1 t /5-3/.

Membrane heliostats. To avoid or reduce manufacturing and assembly efforts associated with individual facets and at the same time obtain high optical quality, so-called "stretched membrane" heliostats have been developed. The reflecting surface consists of a "drum", which in turn is composed of a metallic pressure ring with stressed membranes attached to the front and rear side. For this purpose plastic foils or metal membranes are used. In case of metal membranes, characterised by a considerably longer technical lifetime, the front side membrane is covered with thin glass mirrors to achieve the desired reflectivity. Inside the concentrator, a slight vacuum (only a few millibars) is created either by a vacuum blower or a vacuum pump. By this measure the membrane shape is altered so that the even mirror is transformed into a concentrator. Other designs use a central mechanical or hydraulic stamp to deform the membrane. Both configurations are advantageous since the focal length can easily be set and may even be altered during operation. Disadvantageous is the impact of wind on the optical quality of the heliostat and, in the case of using a vacuum blower, the energy consumption of the blower.

Fig. 5.6 shows the example of such a metal membrane heliostat equipped with a simple tubular steel space framework moving with six wheels on a ring foundation for vertical rotation. Two bearings form the horizontal axis. For this type of tracking, forces are introduced into the stable pressure ring far from the rotation axis (approximately 7 m for the illustrated heliostat). The reduced drive torque keeps the gear units small and inexpensive. The concentrator diameter of the heliostat shown (ASM 150) with a mirror surface of 150 m^2 amounts to 14 m. The concentrator thickness is 750 mm and its weight excluding the foundation is approximately 7.5 t.

Heliostat fields and tower. The layout of a heliostat field is determined by technical and economic optimisation. The heliostats located closest to the tower present the lowest shading, while the heliostats placed north on the northern hemisphere (or south on the southern hemisphere) show the lowest cosine losses. Heliostats placed far off the tower, by contrast, require highly precise tracking and, depending on the geographic location, have to be placed farer from the neighbouring heliostats. The cost of the land, the tracking and the orientation precision thus determine the economic size of the field.

The height of the tower, on which the receiver is mounted, is also determined by technical and economic optimisation. Higher towers are generally more favourable, since bigger and denser heliostat fields presenting lower shading losses may be applied. However, this advantage is counteracted by the high requirements in terms of tracking precision placed on the individual heliostats, tower and piping costs as well as pumping and heat losses. Common towers have a height of 80 to 100 m. Lattice as well as concrete towers are applied.

The costs for piping or the technical challenge of a thermal engine mounted on top of the tower can be avoided by a secondary reflector installed on the tower top, which directs incident radiation to a receiver located at the bottom (beam-

down principle). Although this measure helps to reduce costs for tower, piping and thermal engine, the overall efficiency of the heliostat field is reduced due to additional optical losses caused by the secondary reflector.

Receiver. Receivers of solar tower power stations serve to transform the radiation energy, diverted and concentrated by the heliostat field, into technical useful energy. Nowadays, common radiation flux densities vary between 600 and 1,000 kW/m^2. Such receivers are further distinguished according to the applied heat transfer medium (e.g. air, molten salt, water/steam, liquid metal) and the receiver geometry (e.g. even, cavity, cylindrical or cone-shaped receivers) /5-4/, /5-5/. In the following, the main technical developments are presented according to the applied heat transfer medium.

Water/steam receiver. The first solar tower power stations (e.g. Solar One in California, CESA-I in Spain) have been designed with tube receivers. Their design corresponds to a large extent to the salt tube receiver shown in Fig. 5.7. Similar to conventional steam processes, water is vaporised and partly superheated in such a heat exchanger (i.e. tube receiver). Since superheating is prone to unfavourable heat transmission, and due to the fact that start-up operation or part-load operation require complicated controls, this approach is currently not developed further. The above-mentioned difficulties can partly be prevented by avoiding superheating (i.e. saturated steam is generated). However, under these circumstances the power plant process only allows for comparatively low efficiencies due to thermodynamic constraints.

Salt receiver. The difficulties of heat transmission with a vertical tube receiver, exemplarily shown in Fig. 5.7, can partly be avoided by an additional heat transfer medium circuit. The heat transfer medium applied for this secondary circuit should have a high heat capacity and good thermal conduction properties. Molten salt consisting of sodium or potassium nitrate ($NaNO_3$, KNO_3) complies with these requirements. For both options, thanks to good thermal conduction properties, the heat transfer medium additionally serves as storage medium and can thus compensate fluctuations of the available radiation. The heat of this heat transfer medium is then incorporated into the thermal process via corresponding heat exchangers.

One disadvantage of all such salt receiver is that the salt must be kept liquid also during idle times when there is no solar radiation. This requires to either heat the whole part of the installation that is filled with salt (including, among other components, tanks, tubes, valves) and thus increases the energy consumption of the plant itself, or to completely flush the salt circuit. The highly corrosive gas phase of the used salts also has a detrimental effect, since, for certain operations, undesired evaporation of small amounts of salt due to local overheating cannot be entirely ruled out.

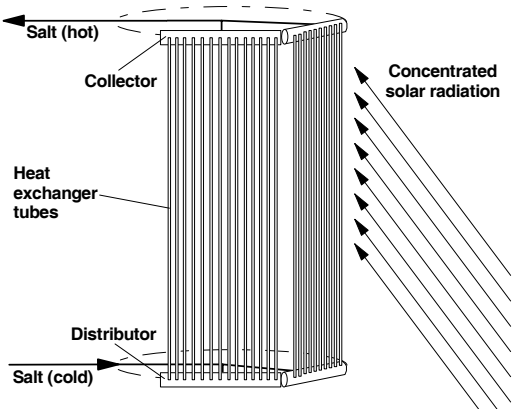

Fig. 5.7 Vertical tube receivers using salt as heat transfer medium

As an alternative to salt tube receivers also salt film receivers may be applied. During this process either molten salt is directly exposed to concentrated solar radiation or a flat or cavity absorber is cooled by an interior salt film /5-6/, /5-7/.

Besides molten salts, generally also liquid metals, such as e.g. sodium (Na) can be applied. However, due to negative experiences made with this heat transfer medium (fire hazard), this approach has been discontinued.

Open volumetric air receiver. Concentrated solar radiation is incident on volumetric absorber material consisting of steel wire or porous ceramics. Such volumetric receivers are characterised by a high ratio of absorbing surface to flow path of the absorbing heat transfer medium air. Ambient air is sucked in by a blower and penetrates the radiated absorber material (Fig. 5.8). The air flow absorbs the heat, so that those absorber areas facing the heliostat field (i.e. illuminated by the solar radiation reflected by the heliostats) are cooled by the inflowing air. Due to this cooling effect the absorber areas radiated by solar radiation are cooler than the interior absorber areas where the heat is transported by the in-flowing air. Therefore the air leaving the absorber shows also a higher temperature compared to the temperature of the absorber areas radiated by solar radiation. This is the reason why this receiver type presents comparatively low thermal losses. Being an open receiver, such power plants operate with ambient pressure. As air is characterised by a relatively low heat capacity, large volume flows and absorber surfaces are required.

Air as heat transfer medium presents the advantages of being non-toxic, non-corrosive, fire-proof, everywhere available and easy to handle. Its disadvantage is its comparatively low heat capacity requiring large heat transmission surfaces which, however, are generally feasible with volumetric receivers. Their lower thermal masses ensure a smooth start-up of the plant.

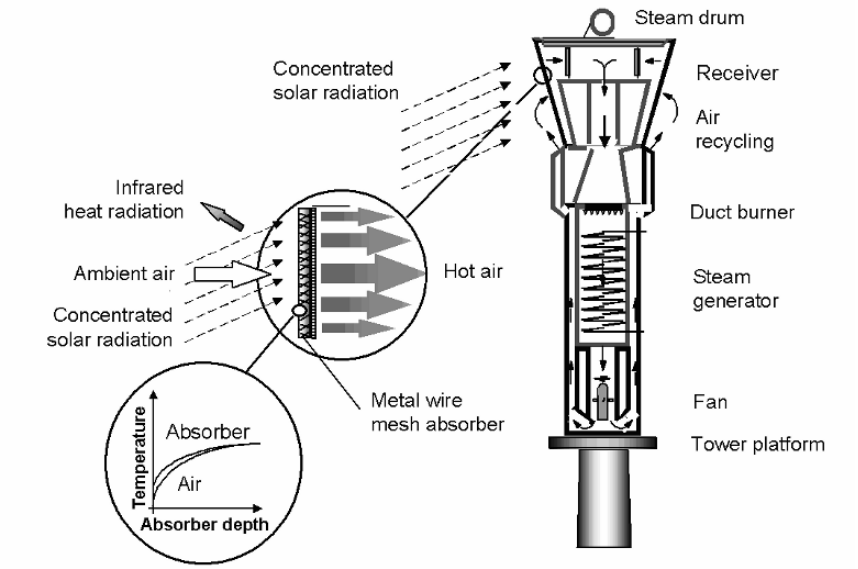

Fig. 5.8 Open volumetric air receiver according to the Phoebus principle (see /5-8/)

Closed (pressurised) air receivers. Receivers of solar tower power plants may also be designed as closed pressurised receivers. The aperture of such receivers is closed by a fused quartz window, so that the working medium air may be heated under overpressure and may, for instance, be directly transferred to the combustor of a gas turbine. To date, for example, a group of closed air receivers of a heat capacity of up to 1,000 kW has been tested at 15 bar. The obtained air outlet temperatures are slightly above 1,000 °C /5-9/. The individual receivers have been designed and interconnected according to their different thermal strain. For commercial applications several module groups may be added (Fig. 5.9).

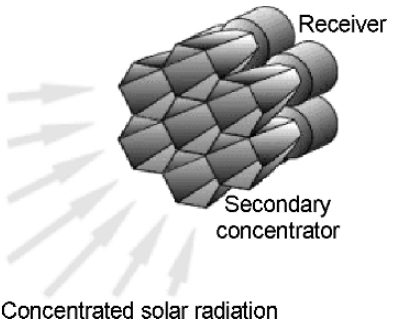

Fig. 5.9 Closed volumetric air receiver cluster equipped with secondary concentrators (see /5-9/)

Power plant cycles. The power plant cycles applied for solar tower power plants are mainly based on conventional power plant components commercially available today; the currently achievable pressures and temperatures of the working media applied for solar tower power plants are in line with the current power plant technology. Solar tower power plants within the capacity range from 5 to 200 MW can thus be designed using commercially available turbines and generators including all required auxiliaries.

5.2.1.2 System concepts

According to the applied heat transfer fluid or working medium, different system concepts are applied. Since open or cavity tube receivers reach working temperatures of approximately 500 to 550 °C, they are predominantly applied for Rankine cycles run by steam. Steam is either generated directly inside the receiver or by the secondary circuit (e.g. molten salt).

Hot air of approximately 700 °C generated by open volumetric receivers can be used within existing steam generators, similar to e.g. heat recovery boilers. The inlet temperature can, for instance, be maintained constant by an incorporated natural gas-fired duct burner, so that this concept is particularly suitable for hybridisation (i.e. application of solar energy in combination with fossil fuels like e.g. natural gas). Outlet gas/air is re-transferred to the receiver by means of a blower so that at least up to approximately 60 % are re-circulated.

Another possibility is the so called inverse gas turbine process. Within such a cycle an open volumetric air receiver is used and the hot air is directly fed into the gas turbine where the air is expanded /5-10/. One advantage compared to a steam cycle is a much simpler design. But so far such cycles have only been analysed theoretically.

In the past, several solar tower power plants have been realised within R&D projects sponsored by public money and industry. Within the following explanations some of these research plants are presented.

Solar One. Solar One is a solar power plant of an electric capacity of 10 MW, which was operated from 1982 to 1988 in the Californian Mojave Desert. This plant proved the general feasibility of solar thermal power generation by tower plants at the megawatt scale. Water was used as heat transfer fluid for the receiver. Among other difficulties, the plant showed the problem of maintaining operation when there are cloud passages.

Fig. 5.10 shows the performance characteristics of the Solar One plant as a typical example of performance characteristics of solar tower power plants. According to this figure, electricity is generated from a daily overall direct radiation of 4 to 5 kWh/(m^2 d) onwards. With increasing direct radiation the electricity output increases approximately linearly. The threshold from which electricity is generated, is mainly determined by the water steam tube receiver technology. This

threshold can be lowered by the use of molten salt and volumetric receivers in particular.

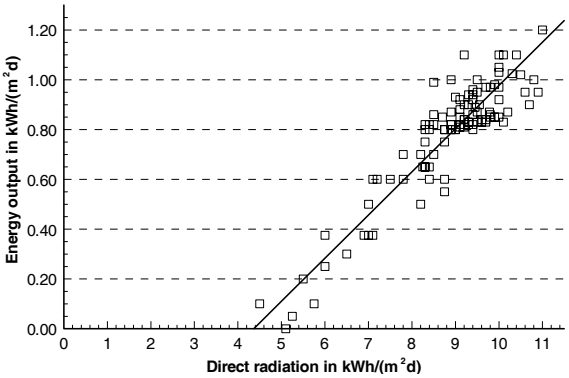

Fig. 5.10 Performance characteristics of Solar One

Solar Two. With the aim to solve the problems encountered with the Solar One plant the latter was remodelled to the Solar Two plant. As heat transfer and heat storage medium, molten salt consisting of 40 % potassium and 60 % sodium nitrate was applied. Thanks to the use of additional thermal energy storage the system is more independent from the available solar radiation.

The functional principle of the Solar Two power plant is shown in Fig. 5.11. Salt is pumped from a "cold" salt storage onto the tower and transferred from there into the receiver, where it is heated by the reflected solar radiation. Subsequently, it reaches the "hot" tank. Hot salt, and thus energy is taken as needed from the storage facility and pumped through a steam generator that generates steam for a conventional steam turbine cycle. Afterwards, the salt cooled inside the steam generator reaches again the "cold" salt storage.

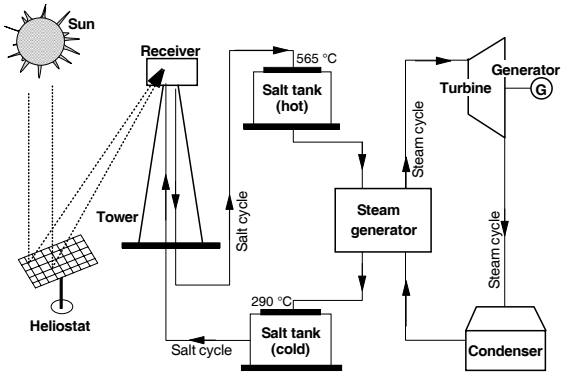

Fig. 5.11 Principle of the Solar Two power plant using molten salt as heat transfer and heat storage medium (see /5-11/)

In principle, this concept allows to generate power not only at daytime but also during the entire course of the day provided that the energy storage and the solar field are sufficiently large. Solar Two shows an electric output of 10 MW which can be maintained up to three hours after sunset thanks to the plant's energy storage.

Phoebus/TSA/Solair. Phoebus/TSA/Solair is a power plant concept with an open volumetric air receiver that provides hot air /5-8/. The hot air is subsequently passed through a steam generator providing superheated steam that can be used to drive a turbine/generator unit. Fig. 5.12 shows the corresponding schematic diagram.

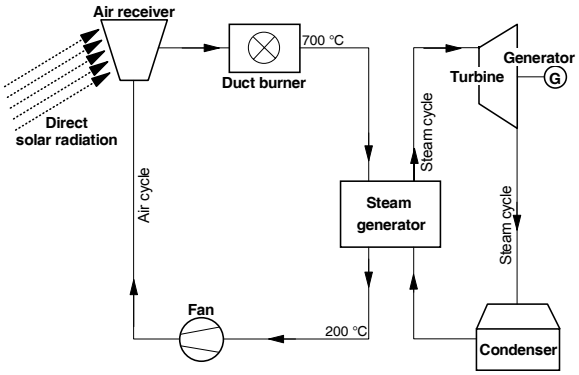

Fig. 5.12 Schematic diagram of an open volumetric air receiver according to the Phoebus-principle equipped with duct burner for additional fossil fuel firing (see /5-12/)

A natural gas-fired duct burner placed in between the receiver and the steam generator adds heat to the air if solar radiation is insufficient to supply the desired steam quantity. The Phoebus plant can thus not only generate power in times of sunshine but also during spells of bad weather and during the night; power generation is thus not exclusively dependent on the available solar radiation.

From 1993 to 1997 such a cycle equipped with an air receiver and a thermal capacity of 3 MW was continuously operated, containing all components of a future Phoebus power plant (so-called TSA system (Technology Program Solar Air Receiver)). Test results have shown the good interaction of components and the low thermal inertia of such systems which enable fast start-up. Further benefits of this technological approach are a simple structure and the unproblematic heat transfer fluid air /5-13/.

PS10. Because of the good experience made with the Phoebus/TSA/Solair System a European consortium, led by a Spanish company, planned the construction and operation of a 10 MW plant named PS 10, equipped with a volumetric air receiver, in the Southwest of Spain in 2004 /5-14/. However, the concept has been

changed. The plant is now provided with a tube saturated steam receiver which supplies steam of 40 bar and 250 °C.

The northern heliostat field was erected from 2005 to 2006. It consists of 624 faceted glass/metal heliostats (T type) "Sanlúcar 120" of a mirror surface of 121 m^2 each. The cavity receiver is mounted on a tower of an approximate height of 100 m, consisting of four 5.36 x 12.0 m tube panels. The thermal storage incorporated into the plant has a useful heat energy of 20 MWh permitting 30 min of operation at 70 % of load /5-15/. Plant commissioning is scheduled for 2007.

Solar Tres. This plant is based on the know-how gathered during the construction and operation of the Solar Two plant (using salt as heat transfer and heat storage medium). This is why the project is called "Solar Tres" (being the Spanish translation for "Solar Three"). This solar tower power plant provided with a molten salt tube receiver and an electric capacity of 15 MW has been exclusively designed for solar operation. The northern heliostat field has 2,494 heliostats of a surface of 96 m^2 each. The heliostats to be used are of the faceted glass/metal heliostat type (T type) equipped with highly reflecting mirrors in simplified design (solar multiple of 3). It is planned that the receiver will have a heat capacity of 120 MW and be of cylindrical molten salt tube design. The storage (600 MWh) incorporated into the concept is to enable operation using heat from the storage for 16 h /5-15/.

Solgate. Solgate is a pilot solar tower power plant equipped with a closed volumetric receiver, a secondary concentrator and a ceramic absorber of an electric nominal capacity of 250 kW designed for hybrid operation (i.e. combined operation using natural gas and solar radiation). The heliostats arranged in the PSA's CESA-1 field have a mirror surface of 40 m^2 each (solar multiple of 1). To date, operation conditions have permitted air outlet temperatures of up to 1,050 °C and the direct drive of the gas turbine /5-9/

5.2.2 Economic and environmental analysis

The following sections are aimed at assessing solar tower power plants according to economic and environmental parameters.

Economic analysis. Within the scope of the economic analysis, power generation costs will be calculated for the discussed types of solar thermal power plants. In line with the preceding assessment method, applied throughout this book, the costs for construction and operation are determined and distributed in the form of annuities over the technical lifetime of the power plant. On the basis of these annual amortisation costs and the provided electric energy, the electricity generation costs per kilowatt hour are calculated. If not otherwise indicated, a technical lifetime of 25 years for all machine equipment and an interest rate of 4.5 % have been assumed to allow for a comparison with other power generation options.

Since the installation of solar thermal plants only makes sense in areas with a high share of direct radiation, a reference site with a total annual global radiation on the horizontal surface of 2,300 kWh/m^2 and a direct radiation total of 2,700 kWh/m^2 has been defined. Such values can, for instance, be obtained at favourable sites in California or North and South Africa.

Based on these site conditions a 30 MW solar tower power plant provided with an open volumetric receiver is assessed. The corresponding technical data are outlined in Table 5.3. This plant is state-of-the-art in terms of solar tower technology.

Table 5.3 Technical data of the assessed 30 MW solar tower power plant

Nominal capacity	30 MW
Mirror surface	175,000 m^2
Full-load hours	2,100 h/a
Storage capacity	0.5 h
Solar share	100 %
Technical lifetime	25 a

Investments. To date, no commercial solar tower power plant has been put into operation. To estimate the power generation costs, we thus need to revert to the figures published by manufacturing and project development companies. On the basis of these data and the adapted specific costs for the heliostats, the overall investment costs for such a power plant amount to roughly 99 Mio. € (Table 5.4). Within the scope of a sensitivity analysis the influence of investment cost variations on the power generation costs are assessed.

Table 5.4 Mean investment and operation costs as well as resulting power generation costs for the reference solar tower power plant

Nominal capacity	30 MW
Investments	
heliostat field	30 Mio. €
receiver and steam generator system	20 Mio. €
tower	15 Mio. €
other components	20 Mio. €
assembly and commissioning	10 Mio. €
design, engineering, consulting, miscellaneous	5 Mio. €
Total	99 Mio. €
Operation and maintenance costs	1.5 Mio. €/a
Power generation costs	0.13 €/kWh

Operation costs. Annual operation costs comprising the costs for operation and maintenance are estimated at 50 €/kW. In the present case, this corresponds to costs of approximately 8.6 €/m^2 of mirror surface and year (Table 5.4). For the

observed plant, the annual overall operation costs thus amount to approximately 1.5 Mio. €.

Electricity generation costs. On the supposition of the above-mentioned investment as well as operation and maintenance costs, the power generation costs related to the solar tower power plant at the reference site amount to approximately 0.13 €/kWh (Table 5.4).

Power generation costs are largely influenced by the number of full-load hours per year, the investment costs and the mean interest rate. A sensitivity analysis conducted on the basis of these parameters reveals the correlations shown in Fig. 5.13. If investments are, for instance, reduced by 30 % power generation costs are cut down to approximately 0.10 €/kWh.

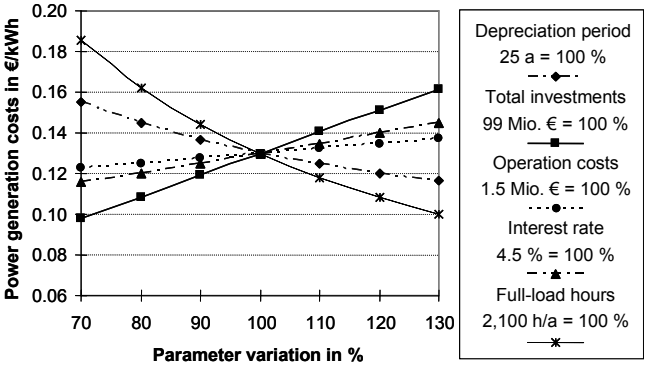

Fig. 5.13 Sensitivity analysis related to the power generation costs of the reference solar tower power plant

However, the sensitivity analysis also shows that for other economic parameters (i.e. higher interest rates, short depreciation period) and different conditions for the particular site, power generation costs can vary significantly.

Environmental analysis. The following analyses are aimed at discussing selected environmental effects with regard to plant erection, normal operation, malfunction, and the end of operation.

Manufacture (construction). Environmental effects related to solar thermal plants may already arise during production of the different plant components. They are to a large share the same as for conventional power plants and other industrial production processes. However, the resulting environmental effects are restricted to very limited periods of time, and in many countries they are subject to extensive legal requirements. Furthermore, solar thermal power plants are primarily located in deserts and steppes where the population density is relatively low. This is why there is so far only a very limited knowledge on the potential effect on human beings and on the environment.

Normal operation. As for all thermal power plants also solar thermal power plants have certain environmental effects during normal operation. In the following, selected aspects are discussed.

- Land requirements. Solar thermal power plants use solar radiation as a source of energy, i.e. an energy source with a comparatively low energy density. This is why such plants necessarily require large collector areas and thus extensive land areas (Table 5.5). Since the individual collectors must be accessible during operation, the soil, where the collector field is installed, is compacted and levelled during construction. Furthermore, highly grown plants may disturb operation and reduce the technical lifetime of the collectors (due to e.g. humidity, shading, and fire hazard). Thus, at the most, grass vegetation is permitted on the respective terrain of e.g. a solar thermal power plant). The soil is therefore more susceptible to erosions. Since solar thermal plants are generally located in areas with little precipitation (i.e. deserts and steppes) and collector fields must be provided with extensive drainage systems to protect foundations and ensure accessibility, this influence can almost be neglected. Due to the glass reflectors, the collector fields are susceptible to damages caused by e.g. extreme winds. The entire plant is thus generally fenced in, so that during the construction of such a solar thermal power plant it has to be ensured that neither natural habitats of large animals nor typical passages are affected. However, due to the preferred location in desert or steppe areas this requirement can generally be fulfilled without any problem.

Table 5.5 Space requirements of solar thermal plants

Tower power plants	20 – 35 m^2/kW
Line-focussing power plants	10 – 25 m^2/kW
Parabolic trough power plant	15 – 30 m^2/kW
Solar updraft tower power plant	approximately 200 m^2/kW
Solar pond power plant	approximately 55 m^2/kW

- Visual impact. Due to their central tower, mainly tower and solar updraft power plants have a non-negligible impact on the appearance of the natural scenery; and the higher the tower the bigger this influence is (approximately 100 m in case of solar tower power plants, and 1,000 m for solar updraft tower power plants). Contrary to wind energy converters, the disturbance of the scenery is static since no moving parts (such as the rotors of wind energy converters) are involved. This is why the impact on the natural scenery is more readily accepted by the spectator. Furthermore, the visual impact can be limited by corresponding shapes and colours as it is presently the case for wind energy converters. At night time, indispensable aviation warning lamps might be perceived as disturbing. Since the tower height amounts to 15 to 25 % of the collector field radius, disturbing shading outside of the plant only occurs with solar altitudes below 15°. Since such plants are preferably built in desert or

steppe areas, due to the low population density, negative optical impacts to humans are hardly to be expected.
- Reflections. Solar tower, trough or dish power plants focus solar radiation onto a particular line or point. Provided that power plants are operated properly, i.e. mirrors are precisely tracking, none of the known environmental effects will occur. However, due to the partly very high energy flow densities of the focussed solar radiation, persons and/or assets may be exposed to considerable hazards in case of improper operation. Proper operation and precise radiation focus of the plants must thus be ensured by all means.
- Emissions. Since some solar thermal power plants also apply conventional power plant technology they are also potential sources of airborne emissions. However, greenhouse gas emissions as well as other types of emissions are only released into the atmosphere during hybrid operation involving fossil or biogenous combustibles. Since the application of these types of fuels is generally subject to extensive legal requirements, environmental effects are usually very limited. Additionally, noise may be created by the turbines and pumps. These sound emissions may be kept to a minimum by appropriate noise protection which has become a state-of-the-art requirement, also with regard to approval according to the existing noise protection regulations, slightly different in different countries. Since the power block is furthermore most commonly located in a central position in the collector field, noise emissions at the facility limits are practically negligible. This is why noise emissions issues have not been reported so far. Further emissions are fumes originating from possible recooling systems of the condensers and the general thermal load of the thermal circuits. But also in this respect, there are extensive legal and regulatory requirements to be fulfilled in order to obtain permission for plant operation.

Malfunction. In case of malfunction, at the most, the same environmental effects as for conventional power stations fired by fossil or biogenous energy carriers are to be expected. Further malfunctions that may arise with regard to solar farms are operating failures due to heat transfer fluid leakage causing personal and environmental damages.

End of operation. To avoid undesired environmental effects, the plants are properly dismantled and discarded at the end of operation. Discarding of the applied plant components should not cause any major environmental effects. They are mostly similar to those of conventional machine technologies, which are relatively low due to the applicable legal requirements.

5.3 Parabolic trough power plants

The line focussing solar fields of parabolic trough and linear Fresnel collectors reflect the incident radiation on an absorber positioned in the focal line of the

concentrator. The collector tracks the sun in one axis (Fig. 5.14). Due to this "one-dimensional concentration" the geometric concentration factors of 15 to 30 are considerably lower than those of two-dimensional collectors discussed above. This is why lower temperatures are achieved when compared to solar tower power plants. However, this disadvantage is compensated by lower specific costs as well as a simpler structure and maintenance.

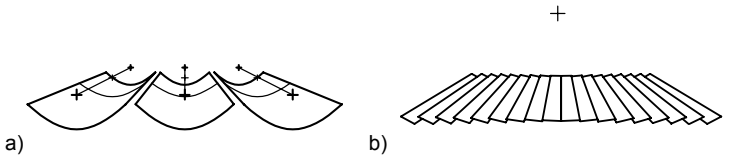

Fig. 5.14 Principles of line focussing collectors (a) parabolic troughs, b) Fresnel troughs)

Line focusing solar power plants have a modular structure. Because of this characteristic and the shape of the solar field, line-focussing solar power plants have in the past also been referred to as "solar farms".

5.3.1 Technical description

In the following, the technology of parabolic trough power plants and Fresnel collector and all related components are described.

5.3.1.1 System components

The system elements composing parabolic trough power plants comprise collector, absorber, heat transfer fluid circuit and power block.

Collectors. The collectors which are typically 100 m, but may nowadays also be 150 m long, are provided with single-axis solar tracking. The annual mean cosine losses of parabolic troughs vary between 10 and 13 %, whereas those of Fresnel concepts are double. After deduction of the optical and thermal losses inside the collector 40 to 70 % of the radiation incident on the mirrors can be used technically. The percentage depends on the design, the field size and on the geographic location of the power plant. In the following, the main collector types are discussed.

Parabolic trough collectors. This collector type is characterised by a parabolic reflector which concentrates the incident radiation onto a tube positioned in the focal line (Fig. 5.14 a), Fig. 5.15, Fig. 5.16).

The reflector itself may either consist of one surface provided with a reflecting layer (metal foil, thin glass mirrors) or of several curved mirror segments arranged in a truss-type structure; the latter variant is commercially applied. Collectors are

mounted on a mounting structure and track the sun's diurnal course by a single-axis system following the longitudinal axis.

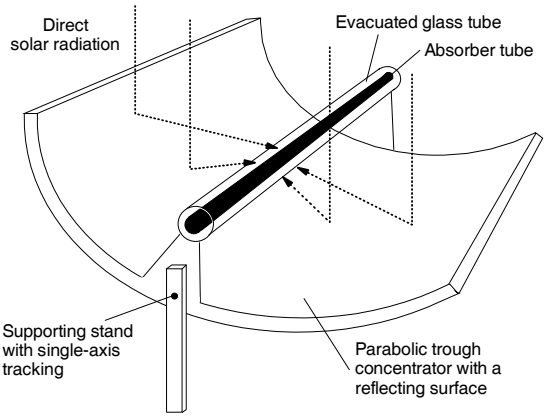

Fig. 5.15 Functional principle of a parabolic trough

The mirror segments typically consist of back-silvered white low iron glass to achieve high reflectivity values in the solar spectrum. When the mirror segments are clean the mean solar reflectivity amounts to approximately 94 %. Since the glass is weatherproof the reflectivity of the cleaned reflector remains practically unchanged.

One collector (SCA = Solar Collector Assembly) is composed of a number of collector elements (SCE = Solar Collector Elements) with a typical length of 12 m each. The largest collector built to date (Skal-ET) consists of 12 SCEs (6 on each side of the central drive pylon). It has an overall length of 150 m and an aperture width of 5.77 m.

Each collector unit is equipped with an angular position sensor to track the position of the collector and optionally additionally with a sun sensor. First electric motors provided with gearboxes or cable winches were used as drives. For the more recent LS-3 and EuroTrough collectors, cost-efficient hydraulic drives have been applied /5-16/.

Fresnel collectors. For this collector type the parabola profile is approximated with individual segments (Fig. 5.14 b)). Individual long rectangular mirror segments of an approximate width of up to 2 m are tracking the sun similar to heliostat fields, so that they reflect the incident radiation to a common focal line. All segments are mounted at the same level (either near-ground or higher on mounting structures). Due to their lower width they are exposed to lower wind loads compared to parabolic trough collectors. However, the different segments shadow each other. Due to their specific geometry, Fresnel collectors are characterised by lower concentrations and a lower optical efficiency when compared to parabolic

trough collectors. Such losses may at least partially be compensated by alternating mirror positions.

Each reflecting segment rotates around its centre of gravity. Segments are actuated either individually or as a group. Fresnel collectors thus require a more sophisticated control system than parabolic trough collectors since a specifically higher number of drives must be used. This is why Fresnel collectors have to date only been tested on a minor scale and have, also on a minor scale, first been commercially applied since 2004 in Liddell, Australia /5-17/.

Absorber / Heat Collecting Element (HCE). Individual horizontal tubes are used as absorbers in the focal line of the collectors; for Fresnel collectors also tube groups may have to be used due to their wider focal line. Today's stainless steel absorber tubes of parabolic trough collectors (i.e. Heat Collecting Element (HCE)) are enclosed in an evacuated glass tube to minimise heat losses (Fig. 5.16). In case of parabolic trough collectors the vacuum also serves to protect the sensitive highly selective coating. Nowadays, such selective coatings remain stable up to temperatures of 450 to 500 °C; solar absorption is above 95 %, and at a temperature of 400 °C emissivity is below 14 % /5-18/.

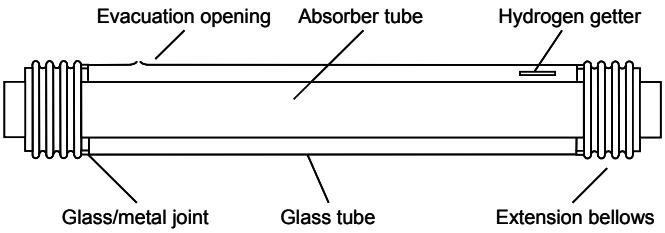

Fig. 5.16 Absorber tube of a parabolic trough collector

In addition to the proven HCE design (Fig. 5.17 a)), Fig. 5.17 b) and c) show two additional variants using a secondary concentrator and a tube bundle receiver. Both options have been proposed to suit the optics of Fresnel collectors.

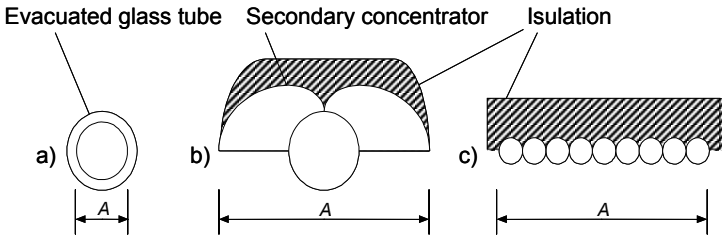

Fig. 5.17 Design principle of receivers of parabolic trough collectors (a); see also Fig. 5.16) and Fresnel collectors b) and c)) (*A* width of the focal line)

Heat transfer medium. To date, high-boiling, synthetic thermal oil has been applied as heat transfer medium in the absorber tubes. Due to the limited thermal stability of the oil, the maximum working temperature is limited to scarcely 400 °C. This temperature requires to keep the oil pressurised (approximately 12 to 16 bar). This is why collector tubes as well as expansion reservoirs and heat exchangers must be of pressure-resistant design. Relatively high investments are thus required.

Hence, as an alternative, molten salt has been proposed as heat transfer medium. Molten salt is characterised by the advantages of lower specific costs, a higher heat capacity and thus potentially higher working temperature on the one hand, and by the higher viscosity of the medium and a higher melting temperature, requiring trace heating, on the other hand. Due to the higher heat capacity, pumping power requirements are still expected to be lower when compared to thermal oil. To date, only prototypes of this variant have been built.

For this reason, investigations of direct steam generation inside the collector tubes are promoted since great cost saving and efficiency potentials are expected. The advantages are the higher possible working temperature of steam as a working medium and that there is no secondary heat transfer fluid loop required including the necessary heat exchangers. The expected problems related to evaporation of water in horizontal tubes (including two-phase flow and thus different heat transmission) can be solved by available technology (forced-circulation boiler with a relatively high recirculation rate and water/steam separator). It is thus possible to directly generate saturated steam by line focussing collectors. However, the high steam pressure (usually between 50 and 100 bar) requires a relatively high tube wall thickness, so that for very wide collectors tube bundles might be more suitable than the well proven individual tube /5-40/.

Collector fields. Nowadays, collector fields are composed of a certain number of loops of an approximate length of 600 m each. These loops are connected to one feed ("cold header") and one discharge line ("hot header") each. Collectors are north-south oriented to allow for high and constant energy yields.

With regard to the collector field design special emphasis must be laid on the distance between the individual collector rows. The distance determines shading during morning and evening hours and thus the corresponding efficiency reduction of the whole field. Furthermore, land and piping costs as well as thermal and pump losses must be taken into account. Since the effect of shading also depends on the latitude, each field design must be optimised with regard to the site-specific conditions. As a rule of thumb, the distance between lines of parabolic troughs typically amounts to three times the aperture width.

Collectors are positioned horizontally; a slope of several percent may also be admissible. However, more severe unevenness of the site must be compensated or terraced.

The achievable thermal output of the entire field is limited by pressure losses of the heat transfer medium and the piping costs. Currently, the maximum economi-

cally sensible thermal capacity of a solar field operated with thermal oil is estimated to be around 600 MW.

5.3.1.2 Plant concepts

The major share of solar thermal electricity is generated by means of parabolic trough plants. In the Mojave Desert in California/USA nine so-called SEGS (Solar Electricity Generation Systems) have been erected, whose concept is detailed as follows. Additionally, further approaches are discussed.

SEGS plants. In the years from 1985 to 1991, nine SEGS plants (Table 5.6) accounting for an overall electric capacity of 354 MW were installed in the Californian Mojave Desert /5-19/. All plants have been operated for power generation on a commercial basis ever since.

Table 5.6 Technical parameters of built parabolic trough power plants (also refer to /5-19/)

	SEGS I	SEGS II	SEGS III	SEGS IV	SEGS V
Year of construction	1985	1986	1987	1987	1988
Capacity in MW[a]	13.8	30.0	30.0	30.0	30.0
Status	in operation	in operation	in operation	in operation	in operation
Collector field					
Collector type	LS1 / LS2	LS1 / LS2	LS2	LS2	LS2 / LS3
Number	608	1,054	980	980	1,024
Overall surface[b] in m^2	82,960	190,338	230,300	230,300	250,560
Max. fluid temp. in °C	307	321	349	349	349
Storage capacity in MWh	120				
	SEGS VI	SEGS VII	SEGS VIII	SEGS IX	
Year of construction	1989	1989	1990	1991	
Capacity in MW[a]	30.0	30.0	80.0	80.0	
Status	in operation	in operation	in operation	in operation	
Collector field					
Collector type	LS2	LS2 / LS3	LS3	LS3	
Number	800	584	852	888	
Overall surface[b] in m^2	188,000	194,280	464,340	464,340	
Max. fluid temp. In °C	390	390	390	390	

Max. maximum; temp. temperature; [a] net capacity; [b] overall collector surface.

All SEGS plants are operated with thermal oil which is pumped through the solar field. For the first plant (SEGS I) mineral oil has been selected that can be operated at low temperatures but does not require pressurised operation. The superheating required for steam turbine operation is provided by a natural gas-fired boiler which also ensures constant operation of the entire plant. The applied oil was so cheap that a simple thermal storage of 120 MWh could be added.

For the following power plants both the applied heat transfer fluid and the power plant configuration have been modified. The thermal oil, still in use today,

allows maximum operation temperatures of scarcely 400 °C, but must be kept under a pressure of at least 12 bar.

From plant SEGS VI onwards, additionally a solar re-heater has been integrated which (together with enhanced steam parameters) increased the thermal efficiency of the power cycle from 30.6 to 37.5 % (Fig. 5.19). Fig. 5.18 shows an example of the performance characteristic of this power plant (i.e. the provided electrical energy as a function of direct radiation).

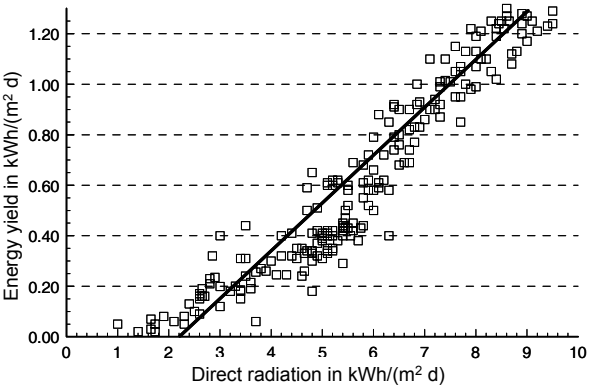

Fig. 5.18 Performance characteristic of the SEGS VI plant

The required steam is either generated directly or indirectly by a secondary circuit (Fig. 5.19). Typical steam parameters are approximately 100 bar / 371 °C for indirect generation (due to the temperature limit of the heat transfer fluid) or 80 bar / 430 °C for direct generation. Compared to conventional steam power plant cycles the indicated values are relatively low. Still, this is to a large extent compensated by an increased technical effort. However, for a plant within this capacity range rather unusual process improvements such as intermediate superheating and multiple-stage internal feed water preheating are required. Consequently, in spite of the rather unfavourable steam parameters, for instance, the 30 MW plants SEGS IV to VI reach thermal efficiencies in the power block of up to 38 %.

Hybridisation is possible by integration of additional firing based on fossil and/or biogenous energy carriers to ensure operation at times of fluctuating or no solar radiation. As an alternative, also parallel steam generators may be applied; this additional technical effort allows for better steam parameters and thus higher electrical efficiencies.

The concept of SEGS plants is also being applied for more recent parabolic trough power plants whose operation is predominantly assured by solar power generation without major additional firing.

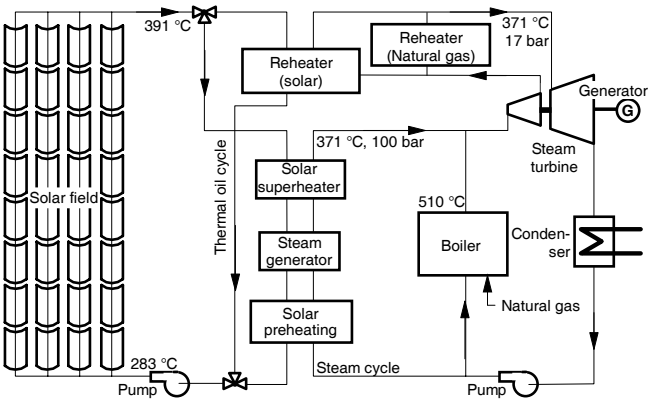

Fig. 5.19 Diagram of a parabolic trough power plant (SEGS VI and VII) (refer to /5-19/)

Integrated Solar Combined Cycle System (ISCCS). To enhance availability, efficiency and controllability, the solar field may be incorporated into a combined cycle power plant. Solar steam is superheated once more up to a temperature of approximately 530 °C in a heat recovery boiler.

If a solar collector field is integrated into the steam cycle of an Integrated Solar Combined Cycle System (ISCCS) the "solar" steam is transferred to the high pressure cycle of the steam generator. The required fossil fuel energy is thus reduced, so that more steam can be generated with the same flue gas stream or less flue gas is required to provide the same quantity of steam. In this operating mode, the gas turbine may be operated at part load; the solar field thus saves fossil fuel energy. The share of solar power generation is between 3 and 10 %.

Integration into conventional power plants. A further possibility to integrate solar heat into conventional power plant processes is to incorporate solar heat into the feed water preheating of conventional steam power plants. For internal feed water preheating, normally turbine extraction steam is required, which is then not available for expansion in the turbine anymore. If solar heat is available for feed water preheating, the steam can be utilised for the turbines.

In summer 2004, the first phase of solar feed water preheating by means of Fresnel collectors was commissioned in Liddell, Australia. For the final configuration it is planned that the last high-pressure pre-heater is exclusively operated by solar heat. In addition, this plant is to be tested with additional steam generation /5-17/.

5.3.2 Economic and environmental analysis

The following explanations are aimed to assess parabolic trough power plants according to economic and environmental parameters.

Economic analysis. Within the following analysis the power generation costs for the outlined solar thermal plants are calculated. In line with the preceding assessment method applied throughout this book, the costs for construction and operation are determined and distributed in the form of annuities over the technical lifetime of the plants. Based on these yearly costs and the provided electrical energy, the electricity generation costs per kilowatt hour are calculated. To allow for a comparison, as usual a technical lifetime of 25 years and an interest rate of 4.5 % are assumed.

Since such plants are only installed in areas with a high share of direct radiation, also a reference site has been assumed, which is characterised by an annual direct radiation total of 2,700 kWh/m^2.

The key data of the assessed 50 MW parabolic trough power plant are outlined in Table 5.7. The plant is defined similar to the AndaSol I power plant /5-15/; differences are due to the selected reference site.

Table 5.7 Key data of the assessed 50 MW parabolic trough power plant equipped with integrated thermal storage

Nominal capacity	50 MW
Mirror surface[a]	510,000 m^2
Full-load hours	3 680 h/a
Storage for 7 h	Molten salt
Solar share	100 %
Technical lifetime	25 years

[a] sufficient for a 80 MW power plant without storage.

Investments. Investment costs for such a power plant vary between 220 and 300 Mio. €. Here a mean of approximately 260 Mio. € is assumed. Specific investment costs therefore amount to 5,200 €/kW, including storage. Table 5.8 shows the approximate distribution of the investment costs.

Table 5.8 Estimation of the investment costs of a parabolic trough solar power plant

Power plant (including thermal balancing)	60 Mio. €
Solar field including heat transfer fluid loop	155 Mio. €
Solar field preparation (i.e. levelling, fencing, access roads)	5 Mio. €
Subtotal (without energy storage)	220 Mio. €
Thermal energy storage (7 h storage)	40 Mio. €
Total	260 Mio. €

Operation costs. Annual operation costs of the collector field are estimated at 5 €/m^2. In addition, there are costs for the remainder of the power plants. All in all, the operation costs for plants of such a size are estimated at 10 €/m^2 of mirror surface and year.

Electricity generation costs. Based on the above-mentioned investment, operation and maintenance costs as well as the possible electricity generation, for the refer-

ence site power generation costs are calculated with 0.12 €/kWh for the parabolic trough power plant with integrated thermal energy storage (Table 5.9).

Table 5.9 Estimation of the power generation costs of a parabolic trough power plant with thermal molten salt storage

Nominal capacity	50 MW
Investment costs[a]	260 Mio. €[a]
Operation and maintenance costs	5.1 Mio. €/a
Electricity generation costs	0.12 €/kWh

[a] including storage.

As for solar tower power plants, not only the full-load hours and the assumed mean interest rate can influence the power generation costs significantly. Therefore a sensitivity analysis is conducted on the basis of these and other parameters. The result of such an analysis show very similar correlations as for the reference solar tower power plant (Fig. 5.13). Accordingly different electricity generation costs are obtained depending on the economic frame conditions and/or the assumed technical parameters.

Environmental analysis. The environmental effects of parabolic trough power plants are very similar to those of solar tower power plants. They are thus discussed in the corresponding chapter on solar tower power plants (see Chapter 5.2.2).

5.4 Dish/Stirling systems

Dish/Stirling systems mainly consist of the parabolically shaped concentrator (dish), a solar receiver and a Stirling motor as thermal engine with interconnected generator.

The parabolic concentrator is tracking the sun in two axes, so that it reflects the direct solar radiation onto a receiver positioned in the focus of the concentrator. The radiation energy transformed into heat within the receiver is transferred to the Stirling motor, which, being a thermal engine, converts the thermal energy into mechanical energy. A generator is directly coupled to the Stirling motor shaft, which converts the mechanical energy into the desired electrical energy (Fig. 5.20). For hybrid operation, the system may be heated in parallel or in addition by a gas burner (operating e.g. by natural gas or biogas).

In the following, the main components of such systems are discussed. Subsequently, the corresponding complete systems are assessed.

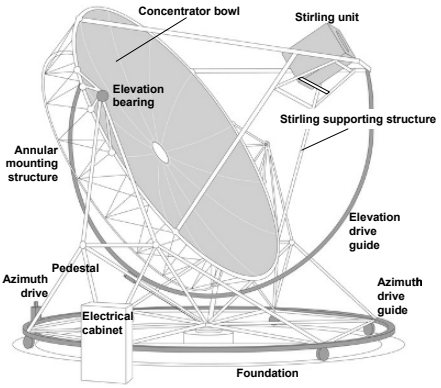

Fig. 5.20 Dish/Stirling systems (Distal II)

5.4.1 Technical description

Within the following explanations, the technology of dish/Stirling power plants including all related components is discussed.

5.4.1.1 System components

Parabolic concentrator (dish). The parabolically shaped concave mirror (dish) concentrates sunlight onto a focal spot. The size of this spot depends on concentrator precision, surface condition and focal distance. Common concentrators achieve concentration ratios between 1,500 and 4,000. Common maximum diameters amount to 25 m.

With regard to concentrator design facetted paraboloids (i.e. consisting of individual segments) and full-surface paraboloids are distinguished.

- For facetted concentrators several mirror segments are mounted on a mounting structure. The segments are supported and oriented individually. Such mirror segments may either consist of glass mirrors or media covered with reflecting foil or thin-glass mirrors.
- For full-surface concentrators the entire concentrator surface is shaped parabolically by a forming process. For instance, a pre-stressed metallic or plastic membrane is attached on both sides onto a stable ring (stretched membrane technology). Subsequently, it is transformed into the desired shape via a forming process (e.g. by water load) and stabilised via a specific vacuum. Such low-weight metal membrane designs provide full-surface concentrators with high rigidity and high optical quality. As an alternative, the facets may also consist of sandwich elements made of fibre-glass reinforced epoxy resin with thin-glass mirrors glued onto them /5-20/.

Mounting structure. The mounting structure of parabolic concentrators is necessarily determined by the shape of the reflector segments or the full-surface concentrator. There is a great variety of technical solutions. However, there is a certain tendency to turntables which at the same time serve as a drive ring. Turntables permit to minimise material consumption and the drive torque.

Solar tracking system. Point-focussing parabolic concentrators must be continuously tracking the sun's path to ensure that solar radiation is always parallel to the optical concentrator axis. Solar tracking systems are further distinguished into azimuth/elevation and polar tracking systems.

- For azimuth/elevation solar tracking, the concentrator is moved parallel to the earth's surface on one axis (elevation axis) and vertically to the earth's surface (azimuth) on a second axis.
- For polar (or parallactic) solar tracking one axis is parallel to the earth's rotation axis (polar axis) and the other vertically to the first (axis of declination).

Both systems are available fully automated. As reference parameter for the control system serve either the solar position, calculated on the basis of date and time of day, or the signal of a solar sensor.

Receiver. The receiver absorbs solar radiation reflected by the concentrator and converts it into technically useful heat. Either the working medium itself or a heat transfer medium may undergo a temperature rise and/or phase change.

Thus, the highest temperatures of the system occur at the receiver. For systems which directly heat the working medium, currently common operation temperatures vary between 600 and 800 °C, whereas pressures are between 40 and 200 bar. Intensity distribution of the focussed radiation within the focal spot cannot be entirely homogenous due to inevitable mirror errors. This is why in addition, large temperature gradients may occur on the absorber surface /5-21/.

Out of the multitude of available receiver technologies, in the following, two different systems are discussed.

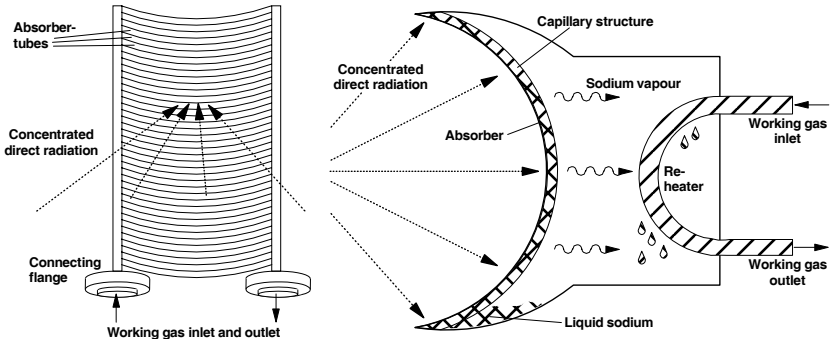

Fig. 5.21 Different receiver types for dish/Stirling systems (left: tube receiver, right: heat pipe receiver, schematic diagrams according to /5-21/)

Tube receiver. The directly radiated tube receiver is the simplest type of a solar receiver suitable for operation with a Stirling motor (Fig. 5.21, left). The heating tubes of the Stirling motor, through which the working medium flows, serve as absorber surface. Thus the receiver tubes are directly heated by the concentrated solar radiation. The volume of the tubes filled with the working medium should be as low as possible to keep the dead volume of the engine low. The shape of the receiver must fit to the geometry of the focal spot produced by the concentrator.

Heat pipe receiver. For heat pipe receivers (Fig. 5.22, right) a phase-change heat transfer medium (e.g. sodium) is applied. Since this heat transfer medium undergoes an evaporation and condensation cycle, the latent evaporation heat is transferred from the radiated absorber surface to the heater and from there to the working medium of the Stirling motor, while the temperature is almost kept constant. Subsequently, the condensate is re-transferred to the heating zone via a capillary structure. Due to the heat pipe principle this structure requires comparatively high efforts in terms of production engineering. However, this concept offers the advantage that high or extremely different heat flow densities may be homogenously transferred onto the Stirling heater thanks to good heat transmission. It is also beneficial that the heat pipe receiver may comparatively easily be combined with other types of operation; i.e. in addition to solar radiation it can also be operated by liquid or gaseous, fossil or biogenous fuels /5-22/.

Such receivers are most commonly designed as cavity receivers. The concentrated radiation passes through a small aperture and impinges on a cavity. The actual absorbing surface, which is subject to temperature rise due to the incident radiation, is positioned behind the focal spot. Because of this geometric position, the absorber surface is bigger than the aperture; the radiation intensity which impinges on the receiver is thus reduced. Yet, with regard to cavity receivers heat losses are relatively low since only a small portion of the diffuse radiation emitted by the absorber is lost by the aperture and convection losses, caused for instance by wind.

Stirling motor. Thermal energy provided by concentrated solar radiation can be converted into electrical energy using a Stirling motor with coupled generator. Stirling motors belong to the group of hot-gas machines and use a closed system; i.e. within the working cycle always the same working gas is used /5-23/. Contrary to Otto or Diesel engines, energy is provided by external heat supply, so that Stirling motors are also suitable for solar operation.

The basic principle of a Stirling motor is based on the effect that gas performs a certain volume change work in case of a temperature change. The process is based on isothermal compression of the cold and isothermal expansion of the hot medium at a constantly low volume, in case of heat supply, and, at a constantly large volume (isochorous), in case of heat removal (Fig. 5.5 (c)). Periodic temperature change – and thus continuous operation – can be ensured by moving the working gas between two chambers of constantly high and constantly low temperature.

For the technical realisation a compression piston is moved to the closed side, so that the cold working gas flows to the warm space, passing through a regenerator. The regenerator transmits the previously absorbed heat to the working gas (isochorous heating phase (1); Fig. 5.22). The gas is warmed up to the temperature of the warm space while the regenerator cools down to the temperature of the cold space. Subsequently, the working gas inside the warm space expands isothermally and absorbs the heat from the warm space (isothermal expansion phase (2); Fig. 5.22).

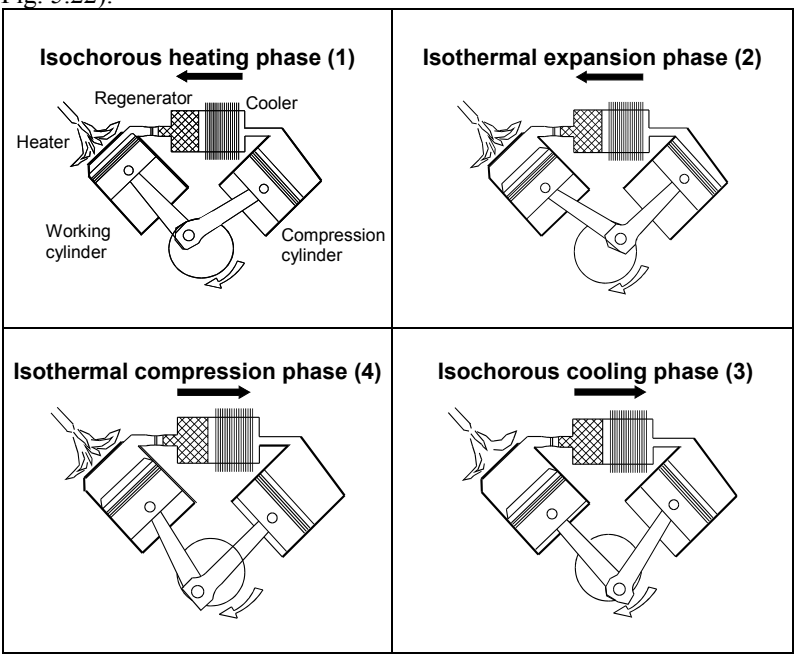

Fig. 5.22 Working principle of a Stirling motor (see /5-24/)

The expanding working gas moves the working piston to the open side and performs work. If the working piston passes the lower dead centre and is thus moved to the closed side, the hot working gas is forced to pass the regenerator and to move into the cold room. Heat is transferred isochorously from the working gas to the regenerator (isochorous cooling phase (3); Fig. 5.22). The gas is cooled down to the temperature of the cold space while the regenerator is warmed up to the temperature of the warm space. The working gas is subsequently compressed isothermally and transmits the generated heat to the cold space (isothermal compression phase (4); Fig. 5.22).

The basic system components thus include the heated working cylinder, the cooled compression cylinder and a regenerator which serves for intermediate energy storage. In most cases, the regenerator is a highly porous body of a high heat capacity; this porous body has a considerably larger mass than the gas mass flow-

ing through the body. The more complete the alternating heat transmission is performed inside the regenerator, the bigger the mean temperature difference between working and compression cylinder and thus the efficiency of the Stirling motor.

If the displacing piston is coupled to the working piston in the appropriate phase angle via a driving mechanism or a vibratory system, the whole system can serve as thermal engine.

In terms of mechanical design, single and double-acting machines are distinguished. In single-acting machines only one side of the compression or expansion piston undergoes pressure fluctuations inside the working space, while the pressure of the working gas is effective on both sides of the piston of double-acting machines; in the latter case, they simultaneously work as compression and expansion piston /5-21/, /5-24/.

Stirling machines can also be distinguished into kinematic and free piston Stirling engines.

- Kinematic Stirling engines perform power transmission via a link mechanism. A generator can be coupled to this gear by a shaft, leading to the exterior.
- Free piston Stirling engines lack mechanical interlinkage between the working piston, the displacement device and the environment. Both pistons move freely. The converted energy can be transferred to the exterior by an axial generator, for instance. Mechanical interlinkage is replaced by an interior spring damping system; this is why only two movable parts are required. The machine is hermetically sealed, so that tightening issues are avoided. Free piston Stirling machines present the theoretical benefits of a simple structure and a high reliability, but are currently far behind in terms of development when compared to kinematic machines.

The machines applied for dish/Stirling systems use helium or hydrogen between 600 and 800 °C as working gas temperatures. Power output of the Stirling motor is controlled by varying the working gas mean pressure.

5.4.1.2 Plant concepts

Because of their size and space requirements individual dish/Stirling systems are suitable to supply power to small and medium grids (micro and mini grids). When combined with batteries and/or additional generators operated by fossil or biogenous combustibles, they are suitable for the energy supply of rural communities. Since, in this respect, they have to compete with a multitude of other renewable sources, current developments concentrate on automated operation and cost-cutting.

Alternatively, dish/Stirling power plants can be interconnected to provide larger quantities of heat and power. The biggest park was commissioned in 1984 in California and consisted of 700 individual collectors and a central thermal engine of an electric overall capacity of almost 5 MW.

In the last years, various dish/Stirling prototypes have been developed and tested. Of some types, several units have been built. Table 5.10 shows the main parameters of the current dish/Stirling plants /5-25/.

Table 5.10 Solar thermal trial and pilot plants (see also /5-25/)

	MDAC	SES/ Boeing	SAIC/ STM	WGA ADDS	SBP	EuroDish
Year of operation	84 – 88	since 98	since 94	since 99	1990 – 2000	since 2000
Capacity in kW_{net}	25	25	22	9	9	10
Efficiency in %	29 – 30[a]	27	20	22	18 – 21	22
Number	6	3	5	2	9	7
Operating hours in h	12,000	25,000	6,400	5,000	40,000	10,000
Availability in %	40 – 84	94			50 – 90	80 – 95
Status	Terminated	Trial run	Trial run	Trial run	Terminated	Trial run
Concentrator						
Diameter in m	10.57	10.57	12.25	7.5	7.5 – 8.5	8.5
Design	1[b]	1[b]	2[c]	3[d]	2[c]	3[d]
Number of facets	82	82	16	24	1	12
Facet size in cm	91 x 122	91 x 122	∅ 300		∅750 – 850	
Mirror support/ Reflector	glass/ silver	glass/ silver	glass/ silver	glass/ silver	glass/ silver	glass/ silver
Reflectivity in %	91	>90	>90	94	94	94 (new)
Concentration factor	2,800	2,800			3,000	2,500
Operation hours in h	175,000	30,000	18,000	54,000	100,000	10,000
Efficiency in %	88.1		90 (design)		88	88
Machine						
Manufacturer	USAB	USAB/SES	STM Corp.	SOLO	SOLO	SOLO
Capacity in kW_{el}	25	25	22	10	9	10
Working gas	H_2	H_2	H_2	H_2	He	He or H_2
Pressure in MPa_{max}	20	20	12	15	15	15
Max. gas temp. in °C	720	720	720	650	650	650
Operating hours in h	8, 000	35,000		80,000	350,000	100,000
Efficiency in %	38.5		33.2	33	30 – 32	30 – 33
Receiver						
Type	tube	tube	tube	tube	tube	tube
Aperture diameter in cm	20	20	22	15	25 – 15	15
Tube temperature in °C	810	810	800	850	850	850
Efficiency in %	90			90	90	90

Max. maximum; temp. temperature; [a] at a gas temperature of 760 °C; [b] facetted glass mirror; [c] stretched membrane; [d] sandwich structure.

Fig. 5.23 shows the example of a typical characteristic power curve for the 10 kW EuroDish plants which have been operated since 2001 in continuous operation (sunrise to sunset) for a total of approximately 10,000 hours (energy and capacity data standardised according to IEA directive /5-21/, /5-25/). According to these figures, the Stirling machine has a shaft power of 11 kW. The tube receiver is cooled by a fan in the overload range at high radiation of over 800 W/m^2.

The concentrator consists of sandwich elements made of fibre-glass reinforced epoxy resin. The segments are assembled to form a closed shell supported by a

ring truss assembly which is characterised by high stiffness and contour accuracy. The front side of the shell is covered with thin-glass mirror to constantly achieve a high reflectivity of approximately 94 %.

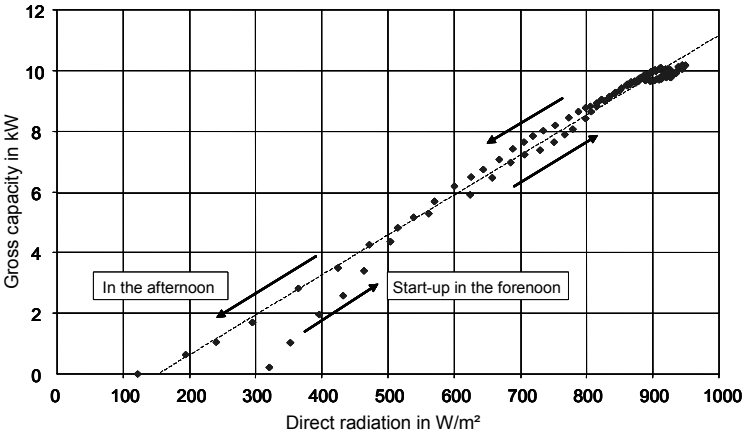

Fig. 5.23 Characteristic curve of 10 kW dish/Stirling systems

5.4.2 Economic and environmental analysis

The following explanations are aimed to assess dish/Stirling systems according to economic and environmental parameters.

Economic analysis. The power generation costs for the described dish/Stirling plants are calculated in line with the assessment method applied throughout this book. According to this, the costs for construction and operation are calculated and distributed in the form of annuities over the technical lifetime of the plant. Specific power generation costs are calculated on the basis of these annual depreciations and the generated electric energy. Unless otherwise indicated, a technical lifetime of 20 years and an interest rate of 4.5 % have been assumed.

Since such plants are exclusively installed in areas of a high share of direct radiation a reference site of an annual direct radiation total of 2,700 kWh/m^2 has been assumed.

The main technical data of the assessed 10 kW dish/Stirling system of the EuroDish type are indicated in Table 5.11.

Investments. Dish/Stirling systems have been tested in continuous operation in the USA and in Spain for more than 15 years. Nevertheless, still they are not commercially available. To approximately quantify the investments, published data of suppliers are used. By doing this we need to bear in mind that the investment costs of trial plants differ tremendously from the values of commercial systems manu-

factured in series. Thus, if serial production of 1,000 systems per year (i.e. 10 MW/a of installed capacity) is assumed, the unit costs for the entire system amount to approximately 45,000 € or 4,500 €/kW plus shipping, assembly, commissioning, planning, engineering and consulting /5-39/. The concentrator including support structure, drive units and foundation contributes for the major share (Table 5.12).

Table 5.11 Technical data of the assessed 10 kW dish/Stirling system (also see /5-38/)

Nominal capacity	10 kW
Concentrator diameter	8.5 m
Full-load hours	2,400 h/a
Storage capacity	none
Solar share	100 %
Solar multiple	1.3
Technical lifetime	20 years

Operation costs. Operation and maintenance costs are estimated to account for approximately 1.5 % of the investment costs (Table 5.12).

Electricity generation costs. Table 5.12 also illustrates the resulting power generation costs. Due to the solar multiple of 1.3 (i.e. concentrator dimensions are sufficiently large that nominal capacity is already reached at mean radiation) the full load hours of the dish/Stirling system of 2,400 h/a are comparatively high in spite of its design without storage. For the outlined reference system specific power generation costs thus amount to 0.18 €/kWh, provided that the investment cost reductions for the assumed 1,000 plants can be reached.

Table 5.12 Investments, operation and maintenance costs as well as power generation costs of 10 kW dish/Stirling power plants

Investments	
mirror, structure, drives and foundation	25,000 €
Stirling motor incl. receiver	11,000 €
transport, assembly and commissioning	4,000 €
planning, engineering, consulting, miscellaneous	6,000 €
contingencies	4,000 €
Total	50,000 €
Operation and maintenance costs	750 €/a
Power generation costs	0.18 €/kWh

As for tower and farm parabolic trough plants, power generation costs are mainly influenced by the achievable number of full load hours, the investments and the assumed mean interest rate.

Environmental analysis. Since the environmental effects of dish/Stirling plants are very similar to those of solar tower power plants, they are discussed within the scope of the corresponding chapters on solar tower power plants (see Chapter 5.2.2).

5.5 Solar updraft tower power plants

For a solar updraft tower power plant the three components of glass roof collector, chimney and turbine are combined. The use of this combination for power generation was already described more than 70 years ago /5-26/.

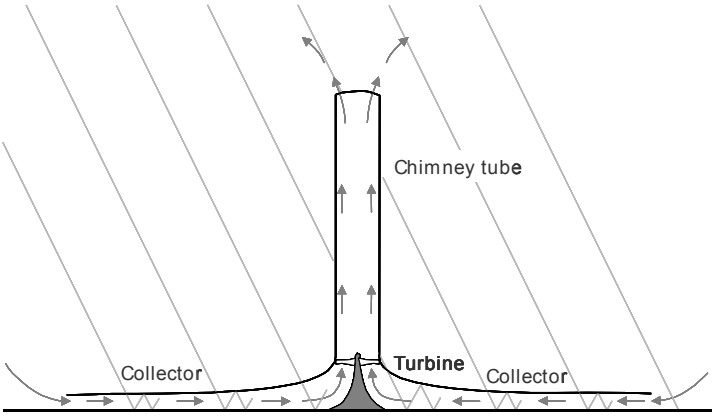

Fig. 5.24 Function principle of a solar updraft tower power plant

The principle, on which a solar updraft tower power plant is based, is shown in Fig. 5.24. The incident direct and diffuse solar radiation warms the air below a flat, circular glass roof, open at the circumference, which, in conjunction with the bottom underneath, forms an air collector. The middle of the roof is equipped with a vertical chimney provided with big openings for air supply. The roof is connected air-tight to the chimney bottom. Since warm air is of lower density than cold air, it rises to the top of the chimney tube. At the same time, the pull of the chimney makes warm air flow from the collector inside the chimney, so that cold ambient air flows inside the collector. Thus, solar radiation ensures continuous updraft inside the chimney. The energy contained in the air flow can be converted into mechanical energy using pressure-staged turbines, located at the bottom of the chimney. Eventually the energy is transformed into electrical energy by means of generators.

The achievable electrical output power P_{el} of a solar updraft tower power plant can be calculated according to Equation (5.6), namely on the basis of the supplied solar energy $\dot{G}_{g,abs}$ and the power plant efficiency η_{PP}. The latter in turn consists of

the efficiency of the components collector η_{Coll}, chimney tube η_{Tower} and turbine(s) $\eta_{Turbine}$ (see /5-29/, /5-30/).

$$P_{el} = \dot{G}_{g,abs} \cdot \eta_{PP} = \dot{G}_{g,abs} \cdot \eta_{Coll} \cdot \eta_{Tower} \cdot \eta_{Turbine} \tag{5.6}$$

The solar radiation supplied to the plant $\dot{G}_{g,abs}$ is calculated according to Equation (5.7) on the basis of the meteorological global radiation incident on the horizontal collector surface $\dot{G}_g$ and the horizontal collector surface S_{abs}.

$$\dot{G}_{g,abs} = \dot{G}_g \cdot S_{abs} \tag{5.7}$$

The impinging global radiation is characterised by a clear diurnal course which also has an effect on the capacity cycle of the solar updraft tower power plant. A balancing of the electric power output of such a power plant – which might be necessary to allow for a more easy integration within an electricity provision system – is possible by an intermediate storage of the solar energy. This is technically possible by black hoses or bags filled with water, which, placed at the bottom of a solar updraft tower power plant, serve as an intermediate storage. During the day the water is heated up inside these storage elements and the stored energy is again released during the night (Fig. 5.25). This measure allows a continuous updraft inside the tower in spite of the fluctuating solar radiation throughout the day, and thus guarantees a continuous power supply (also refer to /5-27/, /5-28/).

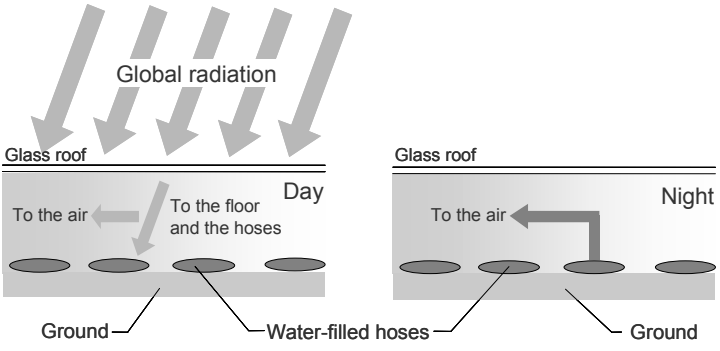

Fig. 5.25 Heat storage by means of water-filled hoses (left: situation during the day; right: situation during the night)

The collector efficiency η_{Coll} is primarily determined by the radiation absorption by the collector and the thermal losses (see Chapter 4.1).

The turbine efficiency $\eta_{Turbine}$ is determined among other parameters by the design of the turbine blades as well as their speed. Profile and tip losses should be minimized. Using multi-bladed turbines with inlet guide vanes (total-to-static pressure) efficiencies of about 80 % can be reached.

Determination of the main parameters of the tower efficiency η_{Tower}, by contrast, is much more complex. For this purpose it is assumed that the tower converts the heat energy supplied by the collector into kinetic energy (convection flow) and into potential energy (pressure drop at the turbine). The difference between the air density inside the tower $\rho_{Air,Tower}$ and the ambient air $\rho_{Air,amb}$ acts as the driving force. The lighter air column of warm air inside a tower of a height h_T is connected to the neighbouring atmosphere at the tower bottom (collector exit and thus tower entry) and consequently gets buoyancy. There is thus a pressure difference Δp between the tower bottom and the environment which is described by Equation (5.8); the pressure difference increases proportionally with tower height. g stands for acceleration of gravity.

$$\Delta p = g \int_0^{h_T} (\rho_{Air,amb} - \rho_{Air,Tower})\, dh_T \tag{5.8}$$

The pressure difference Δp consists of a static Δp_s and a dynamic Δp_d component. The static portion of the pressure difference drops at the turbine whereas the dynamic component describes the kinetic energy of the flow. The distribution of the pressure difference depends on the amount of energy which the turbine withdraws from the flow.

The power contained in the flow P_{Flow} can be described according to Equation (5.9) by the pressure difference Δp, calculated according to Equation (5.8), the flow speed of the air inside the tower v_{Air} and the tower diameter d_T.

$$P_{Flow} = \Delta p \cdot v_{Air} \cdot d_T \tag{5.9}$$

On this basis, the tower efficiency η_{Tower} is calculated as the ratio of the power contained in the flow P_{Flow} (Equation (5.9)) and the power supplied by the collector P_{Abs}, which is calculated by the solar energy supplied to the plant $\dot{G}_{g,abs}$, reduced by the collector efficiency η_{Coll} (Equation (5.10)).

$$\eta_{Tower} = \frac{P_{Flow}}{P_{Abs}} = \frac{P_{Flow}}{\dot{G}_{g,abs} \cdot \eta_{Coll}} \tag{5.10}$$

Inside the collector the flowing air is warmed up by a certain temperature $\Delta\theta_{Air}$ in dependence of the mass flow $\dot{m}_{Air}$ and the specific heat capacity of the air $c_{p,Air}$. On this basis, the thermal power output of the collector P_{Abs} can be calculated according to Equation (5.11).

$$P_{Abs} = \dot{m}_{Air}\, c_{p,Air}\, \Delta\theta_{Air} \tag{5.11}$$

Without the energy extraction of the turbines a maximum air flow $v_{Air,max}$ of the flowing air masses $\dot{m}_{Air}$ is created. Under these circumstances the entire pressure difference Δp is converted into kinetic energy, i.e. the air flow is accelerated. The power contained in the air flow P_{Flow} is calculated according to Equation (5.12).

$$P_{Flow} = \frac{1}{2} \dot{m}_{Air} \cdot v_{Air,\max}^2 \tag{5.12}$$

Under the simplifying supposition that temperature profiles inside the tower and the environment are more or less parallel, the flow speed created at free convection can be expressed by Torricelli's temperature-modified equation (Equation (5.13)); g stands for gravity acceleration, θ_{Air} for ambient temperature of the air and $\Delta\theta_{Air}$ for the temperature rise from the temperature at the collector exit or tower entry.

$$v_{Air,\max} = \sqrt{2\, g\, h_T \, \frac{\Delta\theta_{Air}}{\theta_{Air}}} \tag{5.13}$$

Based on the discussed correlations, the tower efficiency η_{Tower} can also be determined by Equation (5.14).

$$\eta_{Tower} = \frac{g \cdot h_T}{c_{p,Air} \cdot \theta_{Air}} \tag{5.14}$$

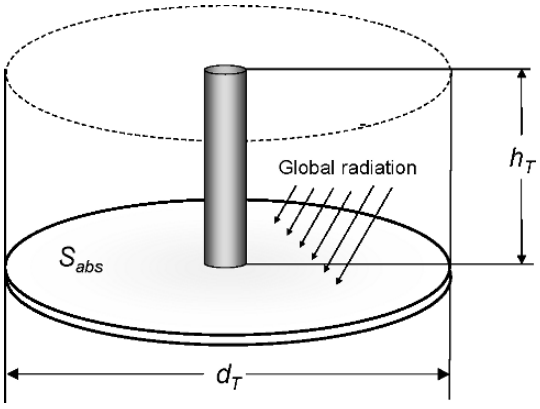

Fig. 5.26 Basic relations of a solar updraft tower power plant

The simplified presentation according to Equation (5.14) reveals that the tower efficiency mainly depends on the tower height. All in all, the power output of the solar updraft tower power plant is thus proportional to the collector surface and to

the tower height (i.e. proportional to the volume of the cylinder shown in Fig. 5.26).

Since the electrical output of a solar updraft tower power plant is thus proportional to the volume of the cylinder created by the tower height and the collector surface, a certain capacity can either be achieved by a high tower in combination with a small collector or by a big collector and a smaller tower. There is thus a "classic" technical/economic optimisation problem to be solved.

5.5.1 Technical description

In the following, the technology of solar updraft tower power plants, including all related components, is described.

5.5.1.1 System components

In the following, the individual components of such a power plant are presented and discussed.

Collector. The hot air required for the operation of a solar updraft tower power plant is created by a simple air collector. The latter consists of a horizontal translucent glass or plastic roof located approximately 2 to 6 m above ground (Fig. 5.27).

The translucent roof is permeable by solar radiation, but impermeable by the long-wave heat radiation emitted by the collector bottom, which is heated up by the sun. This is why the bottom underneath the roof is heated strongly and transmits heat to the air, flowing radially from the exterior to the tower, thereby warming the air.

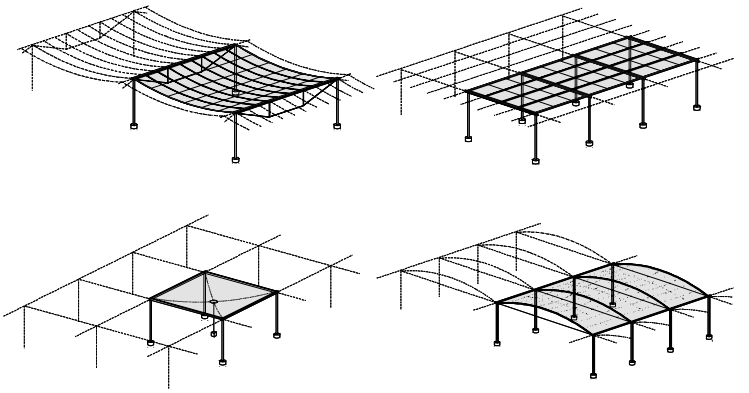

Fig. 5.27 Collector variants suitable for solar updraft tower power plants /5-27/, /5-28/

The height of the air-type collector increases towards the tower. According to this, the flow speed is not increased too much, so that friction losses are kept low. Additionally the losses during the direction change of the air from the horizontal into the vertical direction are minimised.

Storage. If a less pronounced electricity generation peak is desired for the early afternoon, while higher power generation is foreseen for the evening hours, the solar energy can be stored intermediately. For this purpose, water-filled hoses or cushions can be used, which, placed on the collector bottom, considerably enhance the already existing natural heat storage capacity of the ground.

Since already for very low water flow speeds, due to natural convection inside the hoses, heat transfer between the hoses and the water is considerably higher than between the radiation-absorbing surface of the earth (and the soil layers located underneath) below the collector, and also because the heat capacity of water is about five times higher than that of soil, the water inside the hoses stores part of the incident solar radiation. This heat is only released during the night when air temperatures inside the collector are below the water temperature inside the hoses. This is why solar updraft tower power plants can be operated day and night, solely driven by the sun.

Hoses are only filled once and remain sealed afterwards so that no water is evaporated. Depending on the desired performance characteristic the water quantity inside the hoses should correspond to a mean water depth below the collector of 5 to 20 cm (Fig. 5.28).

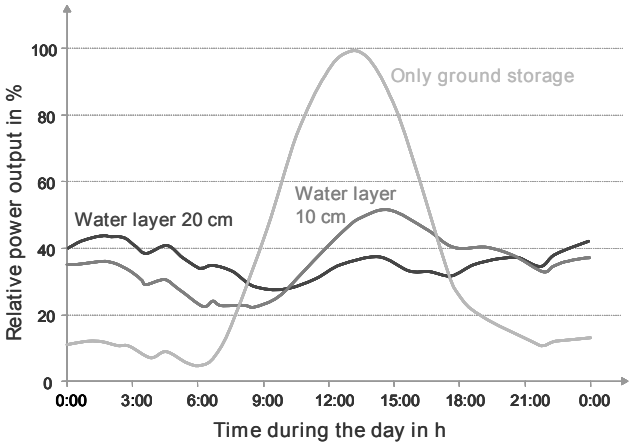

Fig. 5.28 Effect of heat-storing water hoses, located below the collector roof, on the chronological sequence of power provision (simulation results)

Tower. The tower or chimney represents the actual thermal engine of a solar updraft tower power plant. In a first approximation, the updraft of the air heated inside the collector is proportional to the air temperature rise obtained inside the

collector and to the height of the chimney. For instance, in case of a large solar updraft tower power plant ambient air temperature is typically increased by 35 K, so that an air flow speed of approximately 15 m/s is created inside the chimney. Technically speaking, the chimneys of solar updraft tower power plants are very big atmospheric cooling towers.

Towers of a height of 1,000 m represent a great challenge, which is well controlled nowadays. For instance, the high-rise building Burj Dubai, currently under construction, is to be over 700 m high, and for Shanghai a high-rise building of over 800 m is being planned. For a solar updraft tower power plant only a simple hollow cylinder is required. This cylinder does not have a very slim shape and the requirements are considerably lower compared to residential buildings.

Such towers can be built using different technologies; besides free-standing reinforced concrete tubes also steel towers or guyed tower tube designs with sheet or membrane cladding are possible. Studies have shown that virtually for all considered sites reinforced concrete represents the most durable and cost-effective alternative.

For such a tower of a height of 1,000 m the wall thickness is slightly above 1 m at the bottom. This thickness would decrease to approximately 0.3 m at half of the height and remain constant afterwards. Yet, such thin tunnels are deformed by the wind load to an oval cross-section ("ovalisation"). This is particularly true for the suction flanks, represented in Fig. 5.29. Meridional stress becomes very high, so that stiffness is reduced because of cracking and there is also the danger of buckling. Ovalisation can effectively be avoided by bundles of strands in the form of lying spoke wheels stretched across the tower cross-section. They have the same stiffening effect as diaphragms, but reduce the updraft only minimally.

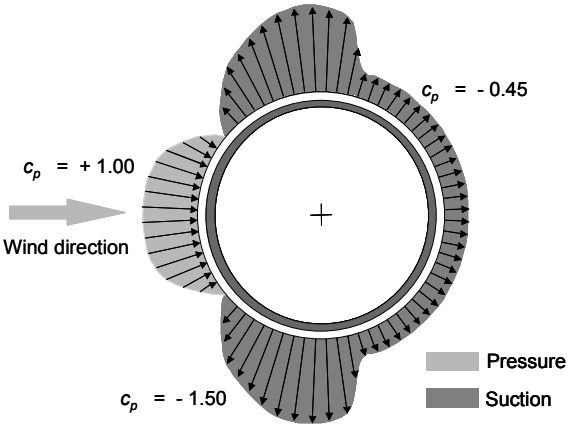

Fig. 5.29 Typical distribution of pressure/suction for the flow around a circular cylinder (c_p coefficient of pressure)

Turbines. Energy is extracted from the air flow by means of turbines. Such turbines to be used for solar updraft tower power plants are not velocity-staged, as

free-running wind energy converters (see Chapter 7.1). They are pressure-staged as cased wind turbo generator sets, and extract static pressure similar to a hydroelectric power plant. Achievable efficiencies are thus higher than for free-running wind turbines.

Air speed in front and behind the turbine is almost the same. The extracted power is proportional to the product of volume flow and pressure drop at the turbine. Turbine control aims at maximising this product for all possible operation conditions.

The pressure drop and thus the flow speed and air flow inside the plant are controlled by the blade adjustment mechanism of the turbine. If, in an extreme case, the blades are at a right angle to the air flow, the power generation is zero. If, for the other extreme position, the air flow passes the rotor unhindered, then the pressure drop at the turbine equals zero; also under these circumstances no power is generated by the rotor. The optimum blade position is between these two positions.

For turbine design, we can revert to the experience gathered with hydroelectric power plants, wind energy converters, cooling tower technology and wind tunnel fans. In this respect, the vertical-axis turbine seems to be the most evident solution. As an alternative, also a larger number of horizontal-axis turbines can be used, placed concentrically in between the collector and the tower, so that cost-effective turbines of common dimensions can be applied.

5.5.1.2 Plant concepts

For research purposes, to date, several very small solar updraft tower power experimental facilities of heights of a few metres have been built (e.g. in the USA, South Africa, Iran and China). However, only one single plant of larger dimensions in Spain has been built and operated for power generation during several years in the 1980s.

Prototype located in the vicinity of Manzanares, Spain. In the years 1981/82, a pilot solar updraft tower power plant of a peak capacity 50 kW was built in Manzanares/Spain (about 150 km south of Madrid/Spain) /5-27/, /5-31/, /5-32/.

This research project was aimed at verifying the theoretical approaches and assessing the impact of the individual components on the capacity and the efficiency of the power plant under realistic technical and meteorological conditions. For this purpose a tower (chimney) of a height of 195 m and a diameter of 10 m surrounded by a collector of a diameter of 240 m was built (Table 5.13).

The chimney comprises a guyed tube of trapezoidal sheets (gauge 1.25 mm, knuckle depth 150 mm). The tube stands on a supporting ring 10 m above ground; this ring was carried by 8 thin tubular columns, so that the warm air can flow in practically unhindered at the base of the chimney. A pre-stressed membrane of plastic-coated fabric, with good flow characteristics, forms the transition between the roof and the chimney.

Table 5.13 Technical data of the prototype in Manzanares/Spain

Tower height	194.6 m
Tower radius	5.08 m
Mean collector radius	122.0 m
Mean roof height	1.85 m
Number of turbine blades	4
Turbine blade profile	FX W-151-A
Tip-speed ratio	10
Operation mode	grid-connected or off-grid
Typical temperature rise in the collector	20 K
Installed name-plate capacity	50 kW
Plastic membrane – collector surface	40,000 m^2
Glass roof – collector surface	6,000 m^2

A variety of types of plastic sheet, as well as glass, were selected in order to establish which was the best – and in the long term, most cost effective – material. It was found that glass is able to withstand even severe storms over many years without damage and proved to be self-cleaning; occasional rain showers were sufficient.

Completion of the construction phase in 1982 was followed by an experimental phase, the purpose of which was to demonstrate the operating principle of a solar updraft tower power plant. The goals of this phase of the project are (1) to obtain data on the efficiency of the technology developed, (2) to demonstrate fully automatic, power-plant-like operation with a high degree of reliability, and (3) to record and analyse operational behaviour and physical relationships on the basis of long-term measurements.

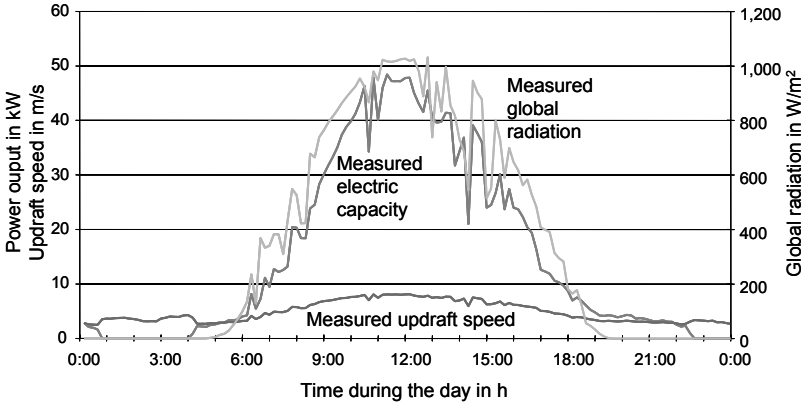

Fig. 5.30 Global radiation, updraft wind speed and power output of the Manzanares prototype (example: measured data at 8th June 1987)

Fig. 5.30 shows selected operational data from Manzanares for a typical day. The data clearly show that for this plant without additional thermal storage the

electrical output during the day closely correlates with solar radiation. Nevertheless, there is a certain updraft that can be utilised for power generation even during some night hours. This becomes also obvious in Fig. 5.31 showing the characteristic curve of such a plant exemplarily for the same day shown in Fig. 5.30. This graphic also outlines that the updraft speed as well as the electrical power provision is directly proportional to global radiation.

In the year 1987, the plant was operated for a total of 3,197 h; this corresponds to a mean daily operating time of 8.8 h. This was achieved by a fully automated plant management which ensured automatic start-up of the plant and synchronisation with the power grid, once the flow speed exceeded a certain value (typically 2.5 m/s).

In spite of the absolutely positive operating results, confirming the calculated data, the test plant was completely dismantled after a storm at the end of the 1980s.

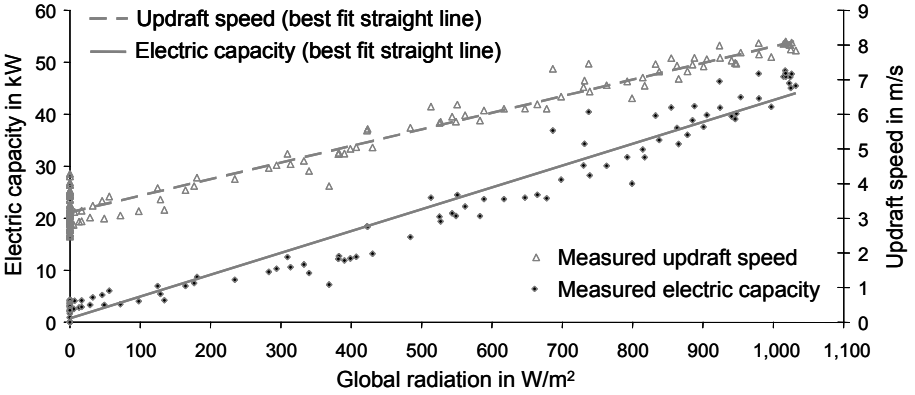

Fig. 5.31 Solar radiation and capacity of the Manzanares prototype (example: measured data at 8th June 1987)

Large solar updraft tower power plants. In spite of the big differences between dimensions of the pilot plant in Manzanares and projected 200 MW plants, thermodynamic parameters are quite similar: Taking, for instance, the temperature rise and the flow speed inside the collector, the Manzanares plant has a temperature rise of up to 17 K and a speed of up to 12 m/s, whereas the calculated mean values for a 200 MW plant are 18 K or 11 m/s /5-33/.

Fig. 5.32 illustrates the results of a simulation calculation of such a 200 MW plant for a site with pronounced seasons. It shows a period of four days for every season. This plant thus also operates night and day without additional heat storage, even though the output power is reduced during the night, especially in winter.

Although various big solar updraft tower power plant projects have been developed, e.g. in India and Australia, to date no commercial plant has been built.

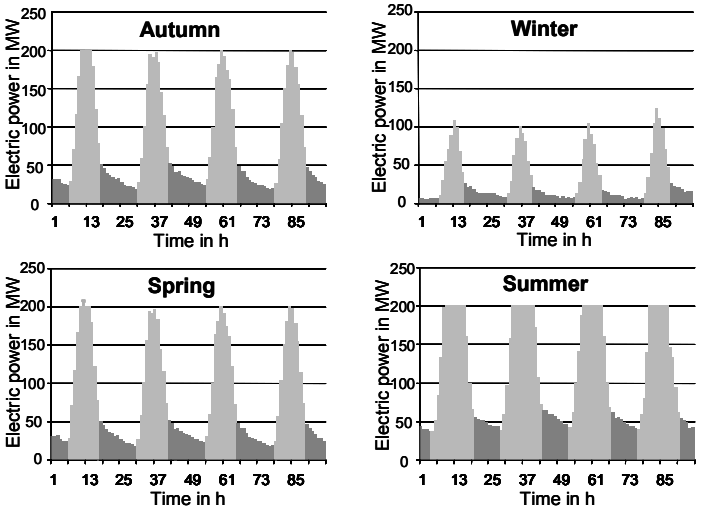

Fig. 5.32 Simulation results for power provision by a 200 MW solar updraft tower power plant without thermal storage

5.5.2 Economic and environmental analysis

The following considerations are aimed at assessing solar updraft tower power plants according to economic and environmental parameters.

Economic analysis. Power generation costs for solar updraft tower power plants are also calculated in line with the method applied throughout this book. Following this, the costs for construction and operation are determined and distributed in the form of annuities over the technical lifetime of the power plant. Power generation costs are calculated on the basis of these depreciations and the generated electrical energy. For this purpose, a technical lifetime of 25 years and an interest rate of 4.5 % have been assumed. In practice, solar updraft towers are designed for longer technical lifetimes (e.g. the tower for 60 years).

Since such plants are only installed in areas with a high share of global radiation, also for this purpose, a reference site characterised by an annual total global radiation on the horizontal plane of 2,300 kWh/m^2 has been assumed.

The energy output of a solar updraft tower power plant is proportional to global radiation, collector surface and tower height. In this respect, there is no physical optimum; thus it is necessary to optimise dimensions according to component costs (collector, tower, turbine) as well as the land costs. This is why plants of different dimensions can be built – at minimised costs – to suit the local conditions at various sites. If the collector surface is cheap and reinforced concrete is expensive, then a large collector and a comparatively small tower will be built.

However, if the collector is expensive, a smaller collector and a bigger tower will be built.

Table 5.14 provides an overview on the typical dimensions of solar updraft tower power plants. The indicated figures are based on internationally common material and construction costs.

Table 5.14 Typical dimensions and power provision of selected solar updraft tower power plants at the reference site

Nominal capacity	MW	5	30	50	100	200
Tower height	m	550	750	750	1,000	1,000
Tower diameter	m	45	70	90	110	120
Collector diameter	m	1,250	2,950	3,750	4,300	7,000
Energy provision	GWh/a	14	87	153	320	680

Investments. Investment costs are determined on the basis of the specific costs and dimensions indicated in Table 5.15. According to this, the investments vary according to the current status of knowledge between 43 Mio. € for a 5 MW plant according to the technical data defined within Table 5.14 and 634 Mio. € for a 200 MW plant (see Table 5.14). However, it needs to be considered that the investment of such plants are afflicted with much more uncertainties than, for instance, conventional power plants, since, to date, no plant of such a size has been built.

Table 5.15 Investment, operation and maintenance costs as well as power generation costs of solar updraft tower power plants

Nominal capacity	**MW**	**5**	**30**	**50**	**100**	**200**
Tower costs	Mio. €	19	49	64	156	170
Collector costs	Mio. €	11	54	87	117	287
Turbine costs	Mio. €	8	32	48	75	133
Engineering, tests, miscellaneous	Mio. €	5	17	24	41	44
Total	Mio. €	43	152	223	389	634
Annuity of investment costs	Mio. €/a	2.3	8.2	12.1	21.2	34.4
Operation and maintenance cost	Mio. €/a	0.2	0.7	1.0	1.7	3.0
Power generation costs	€/kWh	0.18	0.10	0.09	0.07	0.06

Operation costs. The annual operation costs are globally estimated at a lump-sum of 0.5 % of the investment costs. Similar to hydroelectric power plants, operation costs are comparatively low, since the turbines are the only movable components. There are no components that are exposed to high pressures or temperatures. The majority of power plant components is highly durable.

Electricity generation costs. Based on the annual electricity yields determined with simulation models, power generation costs can be calculated; they are within the range indicated in Table 5.15. Following this, they vary between 0.18 €/kWh for the 5 MW solar updraft tower power plant and the order of magnitude of

0.06 €/kWh for the 200 MW plant. Thus, the power generation costs decrease significantly with increasing plant size.

The sensitivity analysis shows similar results as the analysis conducted for a solar tower plant (Fig. 5.13).

Environmental analysis. Environmental effects of solar updraft tower power plants are very similar to that of solar tower power plants. They are therefore discussed within the scope of Chapter 5.2.2 on solar tower power plants.

5.6 Solar pond power plants

Solar ponds are power plants that utilise the effect of water stratification as a basis for the collector. A basin filled with brine (i.e. a water/salt mixture) functions as collector and heat storage. The water at the bottom of the solar pond serves as primary heat storage from which heat is withdrawn. The deeper water layers and the bottom of the solar pond itself serve as absorber for the impinging direct and diffuse solar radiation. Due to the distribution of the salt concentration within the basin, which increases towards the bottom of the basin, natural convection and the ensuing heat loss at the surface due to evaporation, convection and radiation is minimised. This is why heat of an approximate temperature between 80 and 90 °C (approximate stagnation temperature 100 °C) can be extracted from the bottom. Thanks to suitable thermodynamic cycles (e.g. ORC process) heat can then be used for power generation.

5.6.1 Technical description

In the following, the technology of solar pond power plants, including all related components, is explained.

5.6.1.1 System components

As follows the main system components of a solar pond power plant are described in detail.

Pond collector. Pond collectors are either natural or artificial lakes, ponds or basins that act as a flat-plate collector because of the different salt contents of water layers due to stratification. The upper water layers of relatively low salt content are often provided with plastic covers to inhibit waves. This upper mixing zone of such pond collectors usually is approximately 0.5 m thick. The adjacent transition zone has a thickness of 1 to 2 m, and the lower storage zone is of 1.5 to 5 m thickness.

If deeper layers of a common pond or lake are heated by the sun, the heated water rises up to the surface since warm water has a lower density than cold water. The heat supplied by the sun is returned to the atmosphere at the water surface. This is why, in most cases, the mean water temperature approximately equals ambient temperature. In a solar pond heat transmission to the atmosphere is prevented by the salt dissolved in deeper layers, since, due to the salt, water density at the bottom of the pond is that high, that the water cannot rise to the surface, even if the sun heats up the water to temperatures that are close to the boiling point.

The salt concentration of the different layers must thus increase with increasing depth (Fig. 5.33). In a first phase, this ensures stable water stratification. The upper, almost salt-less layer only acts as transparent, heat-insulating cover for the cooling, heat-storing deeper layers at the pond bottom /5-41/.

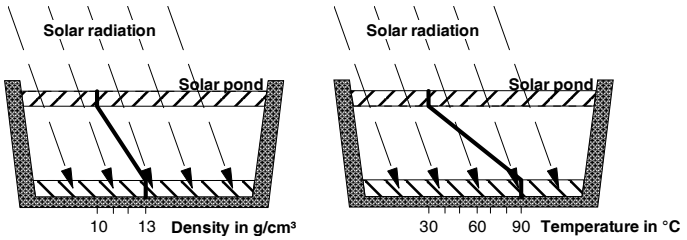

Fig. 5.33 Density (left) and temperature gradient (right) of a solar pond

To ensure stable stratification of a solar pond, with increasing depth the temperature increase must not exceed density increase (i.e. salt content). This is why all relevant parameters must be continuously monitored in order to take appropriate measures (e.g. heat withdrawal, salt supply) in due time.

To achieve the utmost collector efficiency, a high portion of the solar radiation must reach the absorption zone. Yet, this can only be achieved, if the top layers are of sufficient transmission capability.

During the operation of a solar pond, the transmissivity, the salt content and the temperature must be regularly monitored. The timely course of these parameters must be measured from the water surface to the ground in order to determine the heat quantity that can be withdrawn from the pond or to determine the measures to maintain the respective required salt concentration and the water quality (prevention of turbidity due to particulate matter, algae or bacteria).

Diffusion ensures permanent equalisation of the salt concentration in a solar pond which is even intensified by wave motion due to wind near the surface. This is why salt needs to be withdrawn from the surface water and added to deeper layers. For this purpose surface water is evaporated in separate flat basins (salines). Subsequently, the extracted salt is added to deeper zones.

Heat exchangers. Basically, there are two methods to withdraw heat from a solar pond.

- The working fluid of the thermal engine flows through tube bundle heat exchangers installed within the storage zone of the solar pond, and is thereby heated up.
- The hot brine can also be pumped from the storage zone by means of an intake diffuser, subsequently be transmitted to the working fluid of the thermal engine and eventually be re-supplied to greater depths of the pond by another diffuser, once the brine has cooled down. The technical approach allows adjusting the position of the intake diffuser to the depth of the highest temperature. Secondly, heat losses by the pond bottom are reduced, since the cooled water is recycled to the pond near the bottom.

As a matter of principle, a sufficiently dimensioned heat exchanger unit results indispensable for the successful operation of a solar pond. Especially in times of high radiation (i.e. at noon) it has to be ensured that heat can securely be withdrawn from the pond, to prevent phase changes and/or make stratification instable.

Thermal engine. To convert solar thermal energy into mechanical and afterwards in electrical energy, usually ORC processes are applied (see Chapter 5.1.4 and 10.3). These are basically steam cycles which utilise a low-boiling, generally organic, cycle fluid. Such processes permit to provide electrical energy also at low useful temperature differences.

5.6.1.2 Plant concepts

Fig. 5.34 shows the general structure of a solar pond power generation plant. According to this graphic, the water absorbs the incident direct and diffuse radiation, similar to the absorber of a conventional solar collector, and is heated up. The technically adjusted salt concentration prevents natural convection and the resulting heat loss at the surface due to evaporation, convection and radiation.

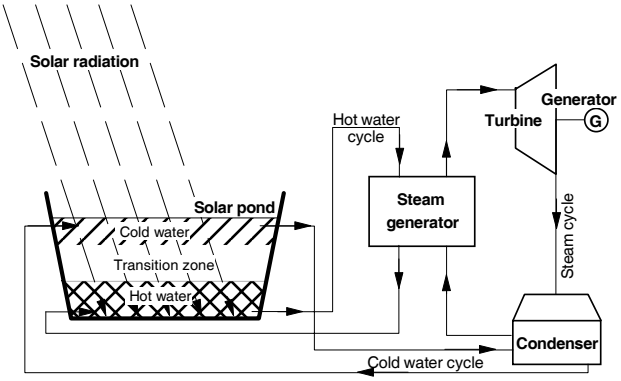

Fig. 5.34 Plant diagram of a solar pond power plant

Water can thus be withdrawn from the storage zone at the bottom at an approximate temperature of 80 to 90 °C. This heat can subsequently be used for power generation by an ORC process.

Solar pond power plants of electric capacities from a few ten kW up to a few MW have been built in Israel, the US (Texas), Australia and India (for process heat provision /5-34/), among other countries. With approximately one percent, solar thermal efficiencies are low; the mean specific capacities range from 5 to 10 W/m^2 depending on radiation, salt content and maximum temperature. For the short-term, also higher capacities can be withdrawn; however, in such a case the solar pond would cool down much faster. Table 5.16 shows typical examples (see also /5-35/, /5-36/, /5-37/).

Table 5.16 Data of selected solar pond power plants

	El Paso Texas, USA	Beit Ha'Arava Israel	Pyramid Hill Australia
Capacity	300 kW_{th} 70 kW_{el}	5 MW_{el} max. 570 kW_{el} (average)	60 kW_{th}
Pond surface	3,350 m^2	250,000 m^2	3,000 m^2

5.6.2 Economic and environmental analysis

The following explanations are aimed at assessing solar pond power plants according to economic and environmental parameters.

Economic analysis. In line with the preceding assessment method, in the following, the power generation costs are calculated for solar pond power plants. According to this, the costs for construction and operation are determined and assessed in the form of annuities. On this basis and the produced electrical energy, the power generation costs are calculated. For this purpose, a technical lifetime of 25 years and an interest rate of 4.5 % have been assumed.

Since such plants are only installed in areas with a high share of solar radiation, a reference site has been assumed which is characterised by an annual total global radiation on the horizontal axis of 2,300 kWh/m^2.

Table 5.17 outlines the main parameters of the assessed solar pond. The solar pond power plant investigated here has a capacity of 5 MW.

Investment costs. Since there are only a few solar ponds, all of them being unique, there are virtually no market prices available that could serve as a basis for these analyses. This is why the following cost estimations have been based on literature values. For this purpose, specific investment costs of 40 €/m^2 of pond surface have been assumed. Literature values are based on cost estimations for civil engineering works and geomembranes; other sources indicate values between 15 and

75 US$/m^2 /5-37/. For the overall plant, in total, specific investment costs of approximately 2,000 €/kW are assumed (Table 5.18).

Table 5.17 Parameters of the assessed solar pond

Nominal capacity	5 MW[a] (peak capacity)
Collector surface	250,000 m^2
Heat exchanger	external; the brine is pumped from the pond and recycled to the pond in cooled condition
Full-load hours	1,150 h/a
Storage	deepest water layer of the pond serves as thermal storage
Solar share	100 %
Net efficiency[b]	1 %

[a] The average capacity amounts to approximately 650 kW; at short-term higher capacities are possible so that higher revenues can be achieved (peak-load power); [b] efficiency between incident solar radiation and produced electric energy.

Operation costs. For this purpose, operation costs are estimated at a lump-sum of 1 % of the investment costs. Besides the maintenance of the heat exchangers and the ORC plant further measures are required since the salt that diffuses from the bottom to the surface has to be retrieved. Compared to conventional steam power plants, the required water quantity is thus many times higher.

Table 5.18 Estimation of the power generation costs of a 5 MW solar pond provided with external heat exchanger

Specific investment costs	2,000 €/kW
Operation costs	100,000 €/a
Power generation costs	0.14 €/kWh

Electricity generation costs. According to Table 5.18, the power generation costs for a solar pond of a surface of 250,000 m^2 and annual operation costs of approximately 100,000 €, amount to approximately 0.14 €/kWh. However, it has been assumed that brine or appropriate salt are available at the site free of charge, so that only transportation measures are required.

For an economic assessment within the scope of operational optimisation, it also has to be considered that electric capacity must be available at any time of the day. Solar ponds can thus generally also serve as peak-load power stations.

Environmental analysis. The environmental effects of solar pond power plants are largely similar to those of solar tower power plants; they are thus discussed in Chapter 5.2.2 on solar tower power plants. Additionally, the salt brine might cause environmental effects when polluting the surroundings of a solar pond. Also, the use of fresh water during the operation of such plants might be considerable. In areas with a shortage of water this could lead to environmental effects.